Pure Appl. Geophys. 179 (2022), 3191–3216

https://doi.org/10.1007/s00024-022-03138-1

Pure and Applied Geophysics

Structure of the Northern Altar Pull-Apart Basin Revealed by a 2D Reflection Seismic Survey: Evolution of the Gulf of California Shear Zone in Northwest Mexico

Jorge Antonio Puente Huerta,[1,2] Mario González-Escobar,[1] and Joann M. Stock[3]

Abstract—The northern Gulf of California and Salton Trough contain segmented marginal basins abandoned during the oblique rift system's evolution during Late Miocene-Early Pliocene. The Altar basin, in northwestern Sonora, Mexico, contains a > 5 km-thick sedimentary record representing the first marine incursion (Late Miocene) of the Gulf of California seaway followed by the first deltaic deposits of the Colorado River. 2D reflection seismic lines were processed and interpreted to characterize tectonostratigraphic features of the transtensional Pacific-North America plate boundary in the northern Altar basin (deep structure, faults controlling the subsidence and accumulation of deltaic deposits). The results show the acoustic basement becoming increasingly shallow toward the northeast, new NW-trending faults, and three major seismic reflectors defining the base of three units: A (oldest), B, and C (youngest). Through similarities in sequence stratigraphy and fauna, we correlate Unit A with the Bouse Formation (SW Arizona and SE California), implying its presence in northwest Mexico. The Altar fault strikes ~ N45°W and aligns with the Dunas fault (SE California), suggesting that these faults are the same continuous structure. Seismic horizons above horizon C are less affected by faults. In contrast, horizons A, B and C are cut by faults, have steeper dips, and are laterally discontinuous. We propose the deposition of unfaulted strata occurred after the latest Pliocene abandonment of the Altar basin. Cessation of major transtensional activity in the Altar basin is coincident with a regional westward shift of transtensional plate boundary deformation, preserving a record of the evolving Gulf of California shear zone in northwest Mexico.

Keywords: Seismic reflection, Altar basin, Cerro Prieto fault, Colorado River delta, Bouse formation, Gulf of California shear zone.

[1] División de Ciencias de la Tierra, Centro de Investigación Científica y de Educación Superior de Ensenada, Ensenada, Baja California, México. E-mail: puente@ig.cas.cz; mgonzale@cicese.mx
[2] Institute of Geophysics, Czech Academy of Sciences, Prague, Czech Republic.
[3] Seismological Laboratory, California Institute of Technology, Pasadena, CA, USA. E-mail: jstock@caltech.edu

1. Introduction

The evolution of the Gulf of California oblique-rift system during the late Miocene to early Pliocene has led to the generation of marginal basins that were segmented and abandoned. Evidence of this evolution is preserved in the Altar basin located in the Sonora, Mexico, and Yuma, Arizona region, which contains a substantial sediment record of the first marine incursion (late Miocene) and the commencement of the construction of the Colorado River delta (Fig. 1) (Helenes et al., 2009; Pacheco et al., 2006). Isolation of the Altar basin, and the northern Gulf of California seaway, from the basins within the Salton Trough was due to the construction of the Colorado River delta; its growth produced lacustrine environments in the north-central part of the Salton Trough that was periodically flooded by discharges of the Colorado River (Dibblee, 1984; Pacheco et al., 2006; Winker & Kidwell, 1996). It is considered that subsidence of the Altar basin ceased due to changes in the location of tectonic activity from the Altar fault to the Cerro Prieto fault. Subsequently, the river diverged from its ancient course and established a course towards the Mexicali Valley (Kinsland & Lock, 2001; Pacheco et al., 2006). Kinsland and Lock (2001) suggest that the ancient Colorado River existed along the Altar basin and entered the Gulf of California at Bahia de Adair (Fig. 1); they consider that the Altar fault may have played a key role during the early definition of the modern transtensional regime, now known to be an important component of the Gulf of California shear zone (Bennett & Oskin, 2014; Bennett et al., 2017).

Reconstructing the Colorado River's evolution is difficult due to the contrasting hypotheses for

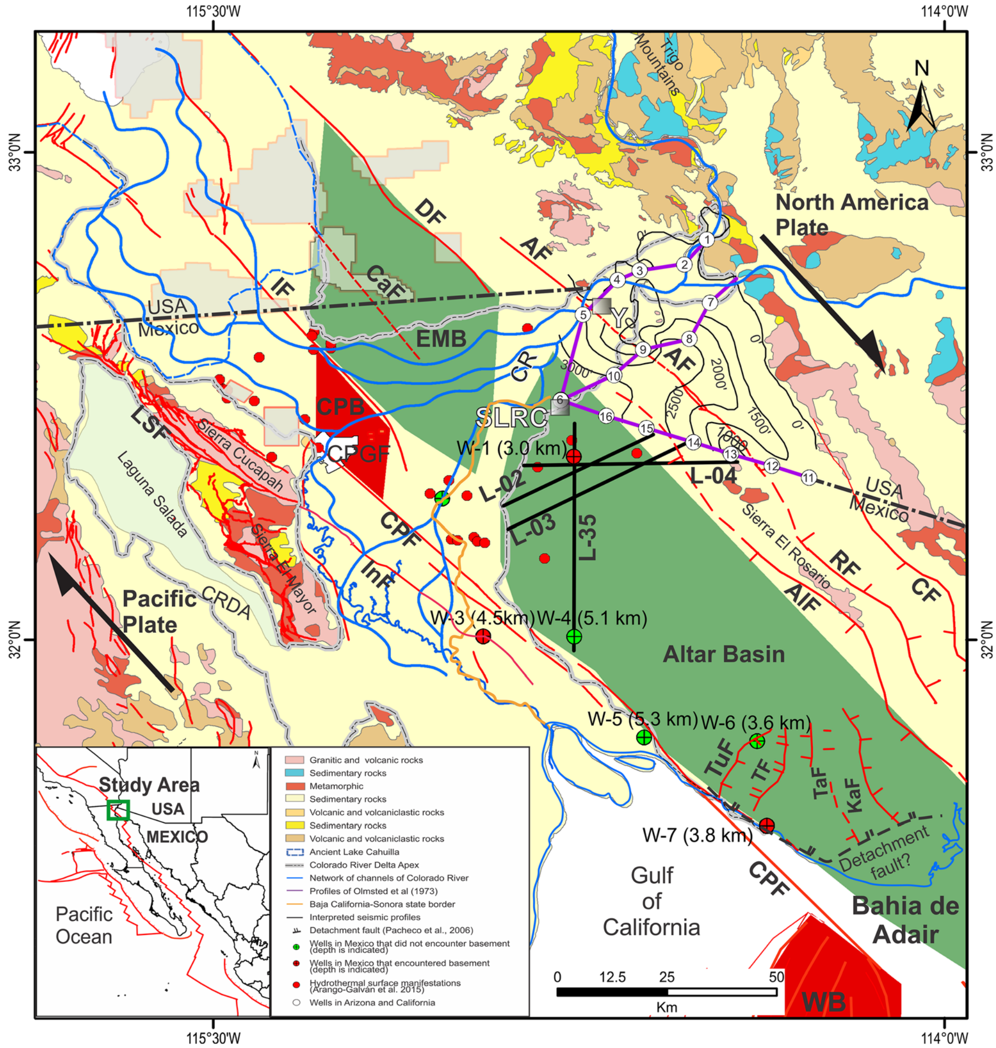

Figure 1
Inset map shows the major tectonic features of northwestern México and southwestern United States and the location of the study area (green rectangle) shown in the main figure. The seismic lines examined in this study are located in the northern part of the Altar basin (black lines). Red lines represent faults. The location of wells (white circles in the USA) and seismic lines (violet lines) and contour lines (depth in feet) of the top of the Bouse Formation from other studies conducted in Arizona, USA adapted from Olmsted et al. (1973). See Table 1 for names and depths of all wells in Arizona and California. Wells in México that penetrated and that did not penetrate the basement are red and green circles with a black cross, respectively, indicating its total depth. Gray polygons with red outline indicate areas of high geothermal potential. *CPGF* Cerro Prieto Geothermal Field. Network of channels of Colorado river including Gila river is shown with blue lines. Color shaded polygons represent inactive (green) and active (red) pull-apart basins bounded by NW-striking strike-slip faults; *EMB*—East Mesa basin, Altar basin, *CPB*—Cerro Prieto basin and *WB*—Wagner basin. *AF*—Algodones fault; *DF*—Dunas fault; *CaF*—Calipatria fault; *IF*—Imperial fault; *CPF*—Cerro Prieto fault; *InF*—Indiviso fault; *LSF*—Laguna Salada fault; *AlF*—Altar fault; *RF*—Rosario fault; *CF*—Caborca fault; *TuF*—Tutuli fault; *TF*—Torres fault; *TaF*—Taracahita fault; *KaF*—Kahwan fault. *CR*—Colorado River. *CRDA*—Colorado River delta area. *SLRC*—San Luis Rio Colorado. *Y*—Yuma. Some faults were taken from Gonzalez-Escobar et al. (2013). The surface geology is from Servicio Geológico Mexicano and GSA-Digital Maps (https://www.geosociety.org/maps/)

depositional paleoenvironments of the late Miocene to early Pliocene Bouse Formation (Dorsey et al., 2018). Since the Bouse Formation is key in understanding the evolution of the river, and considering that Olmsted et al. (1973) reported its presence in the Yuma area, and along the

Table 1

Drilled wells with their total depth (feet) in Yuma, Arizona and California (Fig. 1)

Well number in Fig. 1	Well no.	Name	Total depth (ft)
(1)	(C-7-22)14bcd	USGS LCRP 14	505
(2)	16S/23E	USGS LCRP 23	715
(3)	16S/22E-23Caa	USBR CH-8 RD	360
(4)	16S/22E-29Gca2	USGS LCRP 26	1777
(5)	(C-9-24)8baa	USGS LCRP 28	2466
(6)	(C-11-25)11ab	Yuma Valley Oil and Gas Musgrove 1	4868
(7)	(C-8-22)35caal	USBR CH-704; USGS LCRP 29	1997
(8)	(C-9-22)22cbb	USGS LCRP 25	2318
(9)	(C-9-23)33cdd	USBR CH-20 YM	64
(10)	(C-10-24)24cbb	Colorado Basin Associates Federal 1	6000
(11)	(C-13-20)2abd	USBR CH-28 YM	1427
(12)	(C-12-21)25add	USBR CH-24 YM	410
(13)	(C-12-21)17cbc	USBR CH-23 YM	320
(14)	(C-12-22)9bab	USGS LCRP 24	415
(15)	(C-11-23)34bbc	USGS LCRP 30	623
(16)	(C-11-24)23bcb	USGS LCRP 10	1038

international border (Fig. 1), knowing its spatial distribution and extent south of the Mexico-USA international border towards Sonora, Mexico, is important to understand the paleogeography of this region. However, the Altar basin region is covered by extensive Quaternary sediments and sand dunes that conceal faults and older sedimentary layers that record the late Miocene to Pliocene evolution of this tectonic regime (Chanes-Martinez et al., 2014). Also, during the last 8–12 Myr, the crust has deformed into a wide variety of extensional and transtensional structural styles, which controlled the geometry, subsidence, and sedimentary patterns of the basins. Examination of this oblique rift system provides valuable information on the development of transtensional basins formed along and within the Pacific-North America plate boundary.

Through a cooperative agreement between Petroleos Mexicanos (PEMEX) and the Centro de Investigación Cientifica y de Educación Superior de Ensenada (CICESE), it was possible to obtain access to multichannel reflection seismic and well data in the Altar basin and its surroundings. Pacheco et al. (2006) interpreted six segments of seismic reflection lines; likewise, eight seismic reflection lines were analyzed by Gonzalez-Escobar et al. (2013) to study the structure and seismic stratigraphy to the east of the Altar basin and in the southern part of the Altar basin (Fig. 1). This paper presents a study based on the processing and interpretation of three new seismic reflection lines, the reprocessing and reinterpretation of a seismic reflection line presented in Pacheco et al. (2006), and the integration of data from two wells drilled in the northern sector of the Altar basin (Fig. 1). Additionally, we use existing gravity and magnetic anomalies to interpret the structure of one sector of the Altar basin. We also correlate our interpretation with that reported by Olmsted et al. (1973) to constrain the configuration of the Bouse Formation south of the international border. Finally, we discuss how our results refine and improve the timing and architecture of the Altar basin and its role in the evolving transtensional Gulf of California shear zone.

1.1. Tectonic and Geological Setting

The Gulf of California hosts the tectonic boundary between the North America and Pacific plates and records the late Cenozoic tectonic evolution of northwestern Mexico. The region has evolved from a subduction regime to an oblique continental rift regime that has progressed to an incipient oceanic rift, which has led to the transfer of the Baja

California peninsula to the Pacific Plate by latest Miocene time (ca. 6 Ma; Lonsdale, 1989; Stock & Hodges, 1989; Oskin & Stock, 2003; Oskin et al., 2001).

Crustal extension first occurred over a vast region of northwestern Mexico and formed many mountain ranges and elongated basins with NNW orientations west of the Sierra Madre Occidental. Although no time constraint for the onset of extension has been reported for the area west of Caborca, nor in the Altar basin region (Fig. 1), northwest-trending Basin and Range physiography suggests that this area has experienced a large amount of extension very similar to that of northern Sonora and southwestern Arizona (Pacheco et al., 2006).

This region has been called the Gulf Extensional Province (GEP), which continues to the west to the main Gulf escarpment on the Baja California peninsula (Stock & Hodges, 1989). On the other hand, the eastern limit of the GEP is more complicated to define in the Sonora region due to the overprinting of structures and basins formed during two different stages of crustal deformation; the initial extension of the Basin and Range (Henry and Aranda-Gómez 1992; Stewart & Roldán-Quintana, 1994; Martín-Barajas, 2000; Gonzalez-Leon et al., 2010; Darin et al., 2016), and subsequent right-lateral oblique transtension related to the Gulf of California shear zone and opening of the Gulf of California (Bennett & Oskin, 2014; Bennett et al., 2017; Lonsdale, 1989).

The onset of extension in the Sonora region occurred prior to the oblique rifting of Baja California away from mainland Mexico, with regional extension generating extensional basins with a maximum age for basin initiation constrained to $\sim$ 25 Ma. (latest Oligocene) in the eastern region of Sonora (Gonzalez-Leon et al., 2010). Basin and Range style extension appears to have initiated at a later time in coastal Sonora, occurring 11.7–9.6 Ma (Darin et al., 2016). Locally developing low-angle faults that expose metamorphic core complexes (18 $\pm$ 3 Ma) that were studied in the Mazatán region (Vega Granillo & Calmus, 2003; Wong & Gans, 2003), Magdalena (Nourse, 1989), and southeast of Sonora (McDowell et al., 1997).

1.2. Altar Basin

The Altar basin lies between the town of San Luis Rio Colorado and Bahia de Adair in northwest Sonora (Fig. 1). This area was once part of the Colorado River delta complex, but tectonic deformation raised the surface of the basin, so that now its surface is above the level of the floodplain of the Colorado River and is currently an extensive field of sand dunes (Kasper Zubillaga & Carranza Edwards, 2005; Pacheco et al., 2006). Howard et al., (2015) suggest Pliocene valley aggradation occurred soon after integration of the Colorado River and Gulf of California recorded by the Bullhead Alluvium along most of the lower Colorado River corridor. Altar basin shares a common geological history with other basins within the Salton Trough (e.g., East Mesa and Cerro Prieto, Fig. 1). Each of these basins has experienced the effect of three main tectonostratigraphic events: (1) an initial period of extension and subsidence, in which the Altar fault plays a key role in the Altar basin during late Miocene-Pliocene; (2) an intermediate stage involving one or more episodes of marine sedimentation, which is shown as high-frequency alternation of mudstone, siltstone and sandstone suggesting cyclic processes in the subaqueous part of the delta apron (Pacheco et al., (2006); (3) a final period of basin filling, primarily dominated by the Colorado River delta, and to a lesser extent by alluvial deposits from the basin margins, that is interpreted as a sequence dominated by sandy facies showing progradation of the fluvial facies of the delta in the Altar basin (Pacheco et al., (2006). The ages of the events agree for some areas; however, the beginning and end of sequences differ depending on the basin's relative position to the main depocenter and the configuration of the delta complex. The formation of the Colorado River delta isolated the northern Gulf of California seaway from the basins located within the Salton Trough (Pacheco et al., 2006).

Derived from joint studies of gravity and magnetic data in the basin, the top of basement east of the Altar basin is $\sim$ 3 km higher than within the basin and was interpreted to dip to the west (Sumner, 1972). This basement relief is related to the NW-striking, SW-dipping Altar fault reported from the interpretation of seismic reflection lines, which projects to the southeast into the Gulf of California through the Bahia de Adair region (González-Escobar et al., 2013; Pacheco et al., 2006; Pérez-Tinajero, 2007) (Fig. 1). The southeastern margin of the basin is interpreted to be a detachment fault with a northwest dip (Fig. 1), which was active while most of the sedimentary sequences were being deposited. The Altar fault and the detachment fault may have been kinematically linked to the transtensional domain of the southern end of the San Andreas fault during the late Miocene and Pliocene (Pacheco et al., 2006), likely linking plate boundary structures in the Gulf of California shear zone to those in the eastern California shear zone (Bennett et al., 2017).

Based on well log studies, Pacheco et al. (2006) recognized three principal stratigraphic units that form > 5 km of sedimentary fill in the Altar basin. From oldest to youngest: Unit A, is composed of marine shales 100–900 m thick, with an autochthonous microfauna of possible late Miocene to Pliocene age that nonconformably overlie Cretaceous basement. This unit has been interpreted to represent a shallow marine environment during earliest oblique rifting (Pacheco et al., 2006). Unit B consists of mudstone-sandstone from 1700 to 2200 m thick, sequences that consistently overlap Unit A. Unit B is interpreted to represent transitional environments between the fluviodeltaic facies of the paleo delta of the Colorado River and the marine facies of the northernmost Gulf of California. Unit C is composed of sandstones and conglomerates with a thickness of 1100 m to 3500 m, which overlap Unit B. Unit C is interpreted as deposits of fluviodeltaic channels of the Colorado River (Pacheco et al., 2006).

1.3. Yuma Area and Bouse Formation

The Bouse Formation is an extensive sequence of late Miocene to early Pliocene deposits exposed discontinuously along the southern part of the Colorado River, which varies in thickness and depth. For example, the depth to the top of the Bouse Formation in the subsurface near Yuma, AZ generally deepens towards the southwest (see contours from Olmsted et al. (1973) on Fig. 1). North of the Trigo Mountains (Fig. 1), the Bouse Formation has thickness changes due to syn-depositional fault-related tilting (Dorsey et al., 2017, 2021a, 2021b) This formation represents the conditions and processes that were active during the early evolution of the Colorado River at its southern end and its integration with the Gulf of California (O'Connell et al., 2017; Spencer et al., 2021). The southern part of the Bouse Formation accumulated in a marine environment possibly dominated by ocean tides in the northern part of the Gulf of California (Gardner & Dorsey, 2021; O'Connell et al., 2017; Olmsted et al., 1973). These first marine deposits preceded the formation of the Colorado River delta in the Yuma, AZ area, but higher units from the delta are also included in the southern Bouse Formation (Dorsey et al., 2018).

Debate remains about whether the southern portion of the Bouse Formation, in the Blythe basin, accumulated in a marginal marine estuary or in a large inland lake that was isolated from the ocean (e.g., Spencer and Patchett, 1997; Dorsey et al., 2018; Bright et al., 2018). The Bouse Formation consists of silt and clay, containing fine intercalations of sand and in the basal part sandstone or limestone, tuff and possibly local conglomerate. Invertebrate fossils indicate a brackish, marine environment, but they are not indicators of age. However, the stratigraphic position indicates that the Bouse Formation was deposited in late Miocene to early Pliocene time (Dorsey et al., 2017, 2021a, 2021b; Metzger, 1968; Olmsted et al., 1973). Sr isotopic data are inconsistent with marine water influx and support a lacustrine origin for the Bouse formation (Spencer and Patchett, 1997). Recent studies show that marine waters inundated a former tidal strait in the lower Colorado River valley shortly after the river first ran through it, aided by fault-controlled tectonic subsidence that created and maintained a connection from the lower reaches of the river to the ocean, this tidal strait is related to the deposition stages of the Bouse formation (Dorsey et al., 2021b; Gardner & Dorsey, 2021). Moreover, another recent study concluded that the carbonate member of the Pliocene Bouse Formation in the lower Colorado River Valley southwest of the Colorado Plateau, that has been interpreted previously as estuarine, indicates seasonal genesis in a lake rather than tidal genesis in an estuary in its lamination characteristics (Spencer et al., 2021). As the region we studied is located near the southern Bouse Formation region, it is important to determine if the Bouse Formation is present farther south than presently documented and to constrain its subsurface extent within the Altar basin.

2. Data Analysis

2.1. Seismic Reflection Lines

In the early 1980s, an exploration program was developed by PEMEX in the Altar desert in Sonora, and a 2D multichannel seismic reflection method was applied. The data were collected using an arrangement of 48 channels with a distance of 50 m between receivers. The seismic source used was Vibroseis; the recording time was 5 s with a sampling interval of 4 ms and 4800% redundancy. The processing sequence of seismic reflection data that we applied was as follows (Yilmaz, 2001): (1) editing the seismic traces; (2) filtering; (3) spherical-divergence correction; (4) velocity analysis based on semblance coefficients technique; (5) normal move out and stack; (6) spherical divergence correction; (7) predictive deconvolution; (8) band-pass filtering; (9) time migration; (10) depth migration; and (11) automatic gain control. Following on the work by Puente-Huerta (2019), we conducted processing and interpretation of four seismic reflection lines, totaling 221 km in length, using ProMax and SeisWorks from Halliburton's LandMark software, and OpendTect from dGB Earth Sciences. Two of these lines are oriented SW–NE, one is oriented W–E, and one is oriented N–S (Fig. 1).

2.2. Gravity Anomaly Map

During the interpretation stage, first, we include a Bouguer anomaly map (Espinosa-Cardeña & Elders, 2003) (Fig. 2a), where the highest values are related to structural highs as in the mountainous areas, and the lowest values indicate areas with depressions or basins. We used these gravity data as a guide when we interpreted the position of the top of basement on the seismic reflection lines.

Figure 2 ▶
a Bouguer anomaly over the study area adapted from Espinosa-Cardeña and Elders (2003). Red lines indicate regional faults. Seismic lines used in this study are in the central part of the figure (black lines). Wells in México that penetrated and that did not penetrate the basement are red and green circles with a black cross, respectively, indicating its total depth. CPGF: Cerro Prieto Geothermal field. Small red circles indicate hydrothermal surface manifestations (Arango-Galván et al., 2015). White polygons indicate basins (*EMB*—East Mesa), *CPB*—Cerro Prieto and *AB*—Altar basin. Faults: *IF*—Imperial fault; *CPF*—Cerro Prieto fault; *InF*—Indiviso fault; *Caf*—Calipatria fault; *AlF*—Altar fault; *RF*—Rosario fault; *TuF*—Tutuli fault; *TF*—Torres fault. *CRDA*—Colorado River delta area. Some faults were taken from Gonzalez-Escobar et al. (2013). **b** Magnetic anomaly of the region surrounding the Colorado River delta and Altar basin (Gonzalez-Escobar et al. 2020). Notice the size and locations of magnetic anomalies related to the different structures in the region, particularly the large NW–SE–oriented low magnetic anomaly in the Altar basin (outlined with dotted white lines). *AMD-L*—Aeromagnetic domain low; *CPVC*—Cerro Prieto volcano complex; *CPF*—Cerro Prieto fault; *IF*—Imperial fault; *DF*—Dunas fault; *AlF*—Altar fault; *CF*—Caborca fault; *RF*—Rosario fault; *AF*—Algodones fault; *CaF*—Calipatria fault

2.3. Magnetic Anomaly Map

We use total-field magnetic data that were obtained by the Mexican Geological Survey (Servicio Geologico Mexicano). The contour map of the analytic response (Fig. 2b) shows the region with different magnetization intensities (González-Escobar et. al., 2020). We used these magnetic data to interpret regions of sedimentary basin fill and to identify structures related to basin formation.

3. Results

Analysis of the seismic reflection lines and the Bouger anomaly gravity map yielded interpretations of structural and stratigraphic features, such as faults, zones of deformation, and seismo-stratigraphic events (horizons and acoustic basement). The quality of the data allows reflectors to be resolved down to depths of $\sim$ 5 km, revealing the thickness of the basin and nearby areas.

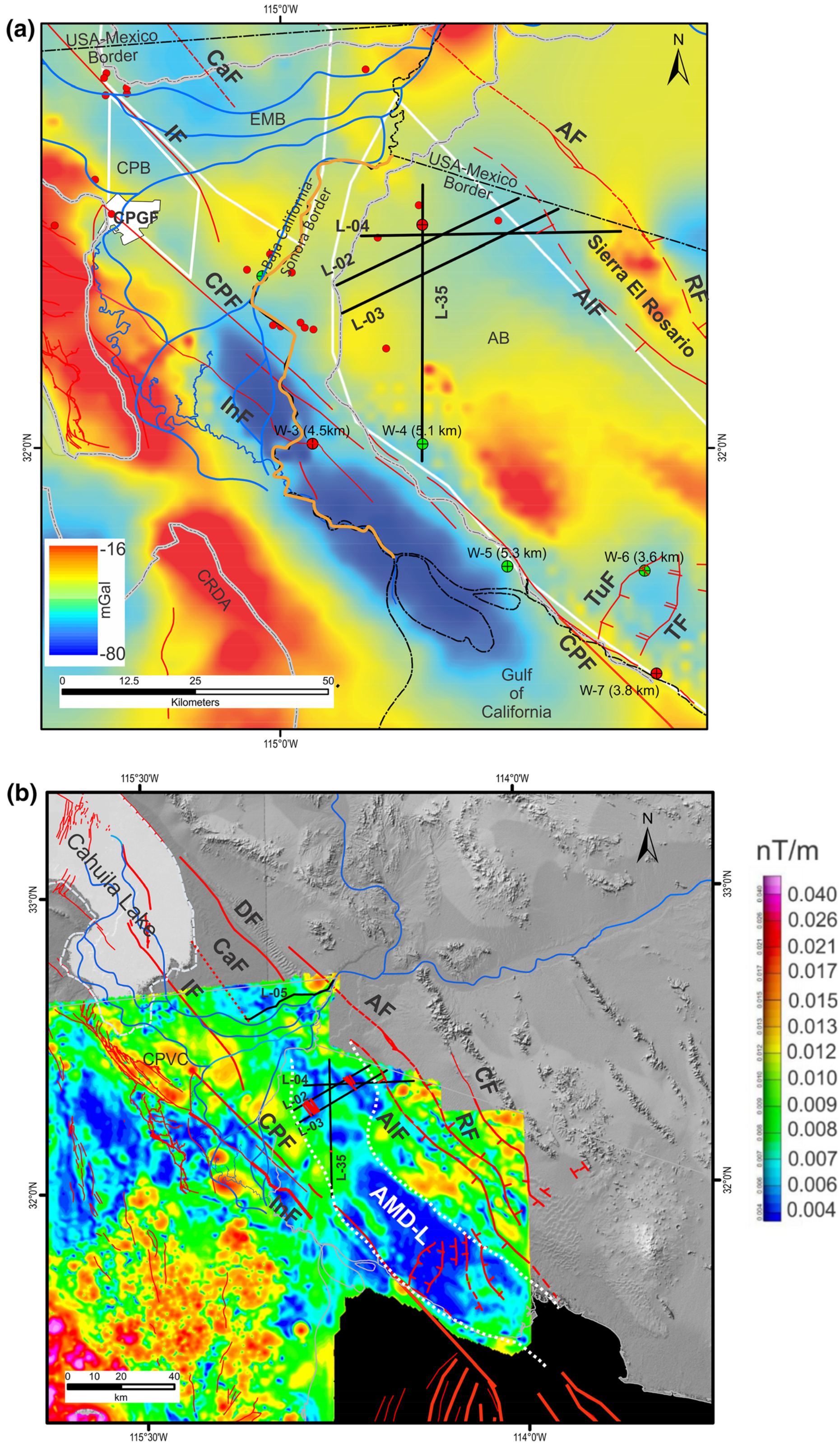
(a)
115°0'W
USA-Mexico Border
CaF
N
EMB
IF
AF
CPB
CPGF
USA-Mexico Border
Baja California Sonora Border
L-04
L-02
L-03
L-35
CPF
Sierra El Rosario
AlF
RF
AB
InF
W-3 (4.5km)
W-4 (5.1 km)
32°0'N
-16
mGal
-80
CRDA
W-5 (5.3 km)
W-6 (3.6 km)
TuF
TF
CPF
Gulf of California
W-7 (3.8 km)
0 12.5 25 50
Kilometers
(b)
115°30'W
114°0'W
33°0'N
32°0'N
Cahuila Lake
DF
CaF
IF
L-05
AF
CPVC
L-04
L-02
L-03
CPF
AlF
RF
CF
L-35
InF
AMD-L
nT/m
0.040
0.026
0.021
0.017
0.015
0.013
0.012
0.010
0.009
0.008
0.007
0.006
0.004
0 10 20 40
km

3.1. Seismic Reflection Lines

Four seismic reflection lines in the northern sector of the Altar basin were processed and interpreted. Seismic line L-35 is oriented in a N–S direction, seismic lines L-02 and L-03 are oriented in a SW-NE direction, and seismic line L-04 is oriented in an E-W direction (Figs. 1, 2). These seismic reflection lines are presented in a color amplitude display that assigns different densities of color (red for positive, and blue for negative) to different seismic amplitude values (i.e. higher amplitude = higher color density), as it allows for better visualization of the structural and stratigraphic characteristics unique to each seismic line.

3.1.1 Seismic Line L-35

Seismic line L-35 is oriented N-S across the northern sector of the Altar basin (Figs. 1 and 2). At its northern end, well W-1 encountered granitic basement at a depth of 2870 m. At its southern end, well W-4 was drilled to 5100 m depth without reaching basement (Fig. 3). This seismic line shows an increase in sediment thickness towards the south based on the continuity of the reflectors along the seismic line. Three primary seismic reflectors are observed, which we correlate to the basal contacts of the three stratigraphic units (A, B, C) previously identified with information from well W-1 and seismic interpretation when this seismic line was first interpreted by Pacheco et al. (2006).

Units A and B (UA and UB) present an irregular seismic pattern, including sub-parallel seismic reflectors that also have an apparent dip to the south. Reflectors in Units A and B have lower impedances (and thus produce lower amplitude reflections) than those in UC. The thickness of UA and UB increases to the south. Farther south on the seismic line, it is not possible to identify the basal horizon of Unit B (HB), nor Unit A (HA). Similar to UA and UB, the thickness of UC increases to the south. The basement is not discernable at depth towards the south.

We map Unit C (UC) on seismic line L-35, which overlies its basal contact, horizon C (HC) (Fig. 3). UC is the thickest unit on seismic line L-35 and is characterized by divergent reflectors, however, the very top of the unit (i.e., HF) has more parallel reflectors and great lateral continuity. The deepest part of this horizon is more challenging to identify. Within this UC, three more distinctive seismic reflectors (HD, HE, and HF) were mapped (Fig. 3). These seismic reflectors have higher amplitudes and greater lateral continuity than the deeper horizons. UC consists mainly of sandstone and conglomerate (Pacheco et al., 2006).

Figure 3 ▶
Seismic line L-35, uninterpreted (**a**) and interpreted (**b**). The seismic horizons A, B, and C, reported by Pacheco et al. (2006), and three more (D, E, and F) above horizon C. Well W-1 (red circle) penetrated the crystalline basement at 2.8 km depth, and well W-4 (green circle) was drilled to a depth of 5.1 km without encountering basement. Red lines are faults. Arrows indicate relative apparent vertical motion. Circle-dot and circle with x indicate suspected strike-slip motion component. HA-represents the top of acoustic basement (green color in all seismic lines). *ArF* Arena Fault; *H*—Horizon; *U*—Unit

Two of the shallowest seismic horizons (HD and HE) are cut by faults defined between km 9 and km 45, while the youngest horizon (HF) does not appear cut by faults in some sectors. A significant fault, which we named Arena fault (Fig. 3), cuts the three seismostratigraphic Units UA, UB, and UC, without affecting the shallowest horizons HE and HF, suggesting that the Arena fault became inactive before deposition of the sediments above HE. However, other faults cut Unit E to the south of the seismic line (between 35 and 46 km). Collectively, these observations constrain the end of tectonic activity in the northern part of the Altar basin to prior to the deposition of Unit F (UF).

3.1.2 Seismic Lines L-02 and L-03

Seismic lines L-02 and L-03 are oriented SW-NE across the northern sector of the Altar basin (Figs. 1 and 2). Due to the proximity and parallel orientation of seismic lines L-02 and L-03, there is a significant similarity in the stratigraphy and structures observed. Seismic line L-02 (Fig. 4) contains the same horizons also interpreted in seismic line L-35 (HA, HB, HC, HD, HE, and HF), all of which have apparent dips to the southwest. On seismic line L-02, HC is not

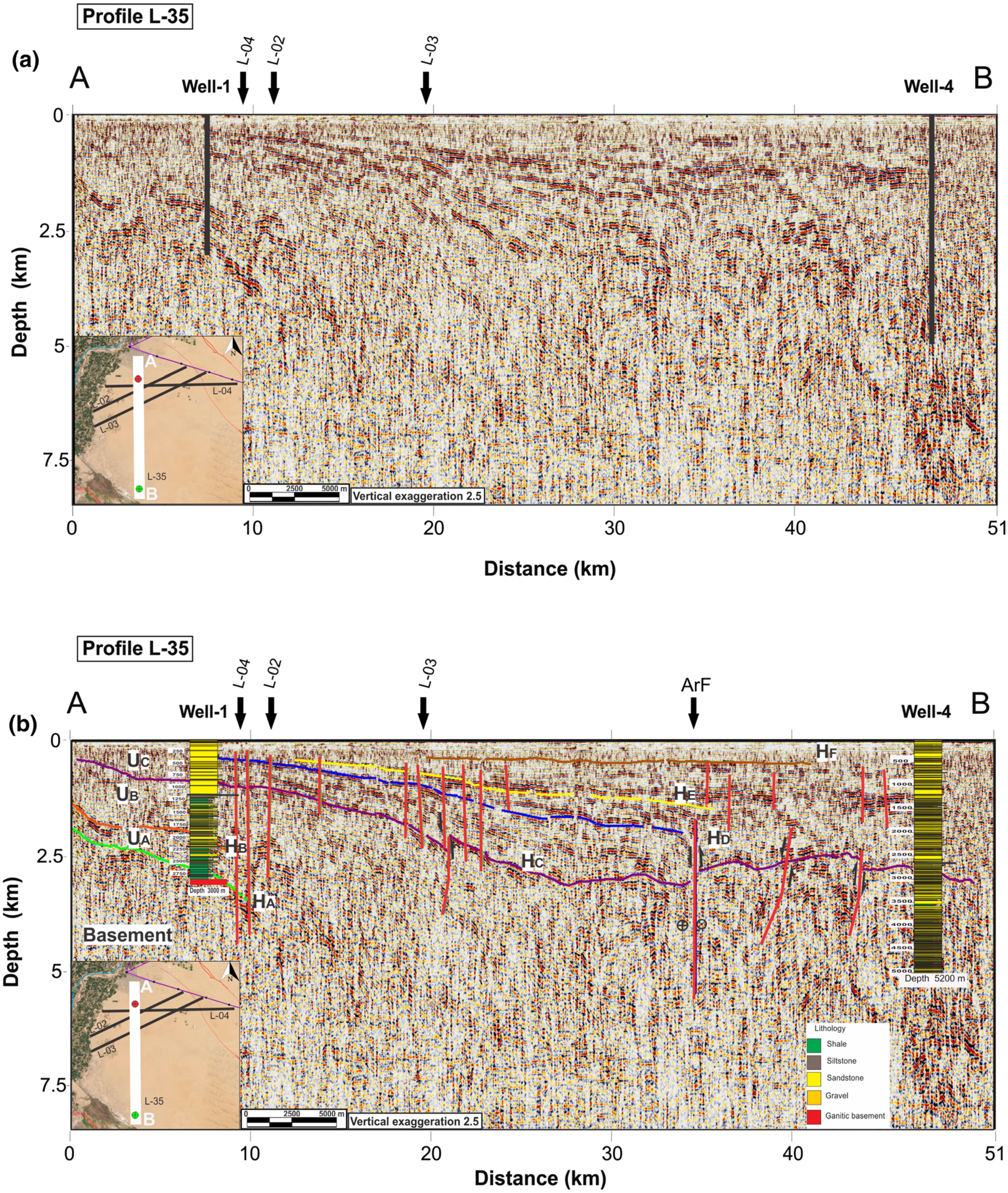

observed below depths of 2500 m, where resolution was poorer. On the northeastern half of seismic line L-02, HA and HB continue to the NE becoming shallower, where they are observed within 650 and 1650 m of the surface, respectively. A seismic reflector (HD) was interpreted in the shallow part between km 6 and km 17.

The HF, in the shallowest part of the section at the southwest end of the seismic line, is cut by a set of faults only observed from ~ 250 m to ~ 1800 m depth. This same horizon is not cut by faults where it is observed in seismic line L-35. In seismic line L-02 (Fig. 4) the faults that cut HF are located 12 km to the west of seismic line L-35, towards the central part of the Colorado River delta region, closer to the Cerro Prieto fault (Fig. 2). In this seismic line, another set of faults is observed, and within this is the San Luis fault (Fig. 4). This set of faults is located between km 19 and km 24, and some faults reach the acoustic basement, as is the case of the San Luis fault, which appears to bound the northeastern margin of a diffuse structural high located between km 16 and km 19 (Fig. 4).

In seismic line L-03 (Fig. 5), as expected, we observe the same structures as in the seismic line L-02 due to their proximity. The apparent southwest dip of HA, HB, and HC is similar to that observed in seismic line L-02. Also, the sedimentary thickness of all units increases towards the southwest.

HA and HB are cut by faults that appear between km 25 and km 40, which accommodate the basement offset. We map the Altar fault near the northeastern end of seismic line L-03, which displaces the top of basement (horizon HA) down-to-the-southwest by approximately 250 m. It was also possible to define the San Luis fault where it offset horizons HA and HB, although it could not be followed to shallower depths because the reflectors are poorly defined above depths of ~ 1000 m. Additionally, the shallowest reflector (HF) is cut by a set of shallow faults at the southwest end of the seismic line, located between km 2.5 and km 8, however, it postdates faulting elsewhere: this could indicate differences in when the tectonic activity became inactive in different parts of the basin.

3.1.3 Seismic Line L-04

Seismic line L-04 is oriented W-E across the northern sector of the Altar basin (Figs. 1 and 2). In this seismic line (Fig. 6), we observed a structural high at the east end of the seismic line, where basement is observed within ~ 430 m of the surface. This high amplitude reflector (HA) is interpreted as the top of acoustic basement, which has an apparent west dip across the Altar basin. This behavior is congruent with the gravity anomaly map that shows higher values towards the east in the Sierra El Rosario (Fig. 2), and the fact that the basement gets shallower to the east and is exposed in the Sierra El Rosario (Fig. 1). On the western side of seismic line L-04, this reflector reaches depths of ~ 5000 m. HB shows a remarkable continuity and apparent dip to the west, similar to the basement surface. The shallow horizons observed on the other seismic lines (e.g., HD, HE, and HF) are not observed on seismic line L-04.

A set of faults was interpreted between km 28 and 36, including the Altar fault (Fig. 6). The Altar fault is recognized by the west-side down basement offset of ~ 450 m. Another important set of shallow faults occurs between km 13 and 20. Some of these penetrate the entire sedimentary package to reach the acoustic basement. Among these, the San Luis fault stands out (Fig. 6), defining the eastern margin of a possible structural high that also affects HB and HA, and is the same relatively deep and subtle structural high observed in this area in seismic lines L-02 and L-03, however, geometry of this possible structural high is not well defined due to poor resolution. It was not possible to follow any seismic horizon deeper than this structure.

Figure 4 ▶
Seismic line L-02, uninterpreted (**a**) and interpreted (**b**). Three strong seismic reflectors are observed, including HA, which separates the basement from the mudstone unit A. Overlying Unit A is HB in orange, and HC in purple, all cut by a series of faults, including the San Luis fault. Upsection, horizon D (HD) is in blue; two higher seismic reflectors in yellow and brown color are cut by shallow faults (HE, HF). Red lines are faults. Arrows indicate relative apparent vertical motion. Circle-dot and circle with x indicate suspected strike-slip motion component. *SLF* San Luis Fault. *Cal-ArF* Calipatria-Arena Fault. *H*—Horizon

3.2. Subsurface Architecture of the Altar Basin

The 3D subsurface architecture of acoustic basement, and thus the floor of the Altar basin, is interpreted from combining interpretations of intersecting seismic lines with constraints from the drill holes located at the north and south ends of seismic

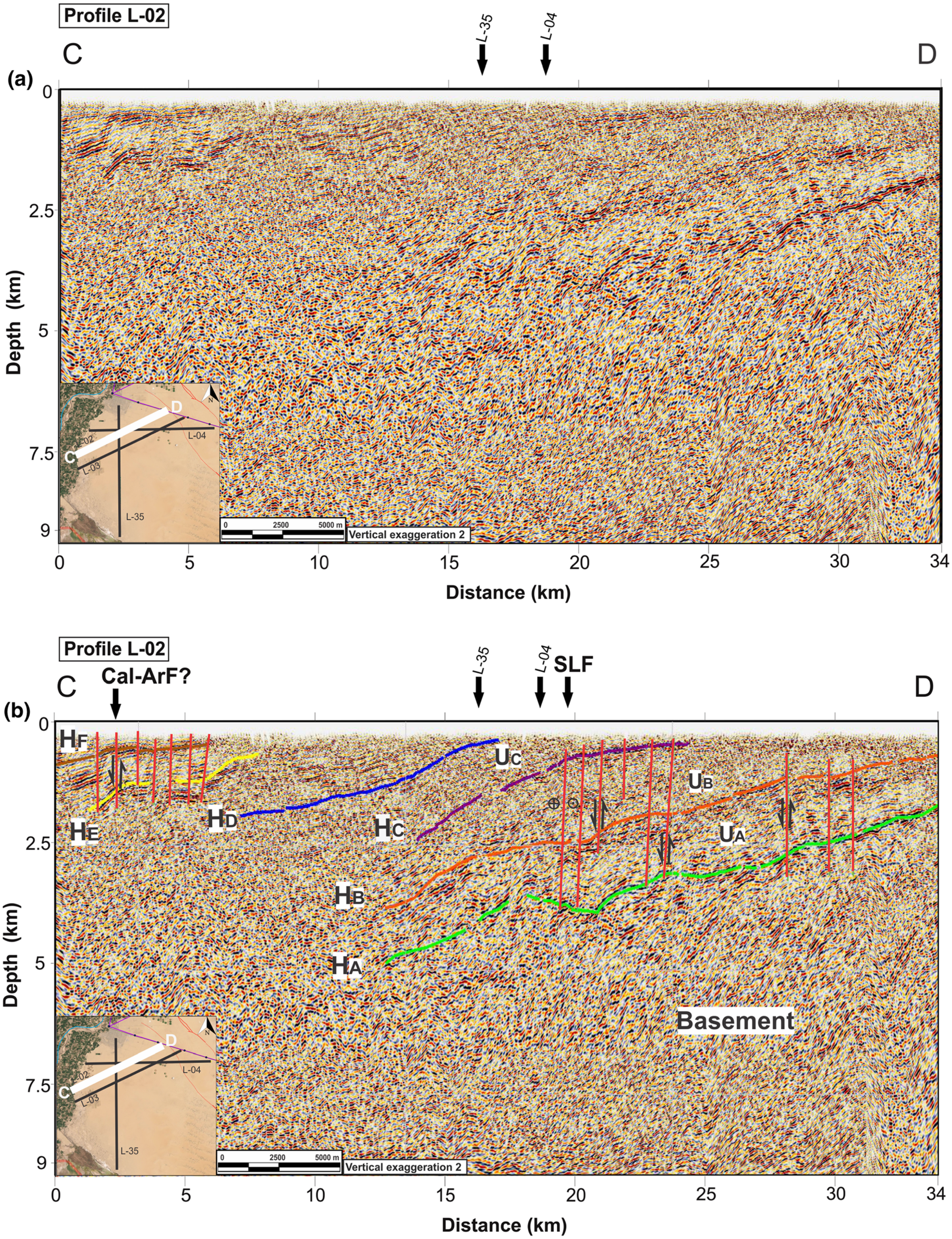
Profile L-02
C
D
L-35
L-04
(a)
Depth (km)
Distance (km)
Vertical exaggeration 2
0 2500 5000 m
Profile L-02
Cal-ArF?
SLF
(b)
HF
HE
HD
HC
HB
HA
UC
UB
UA
Basement

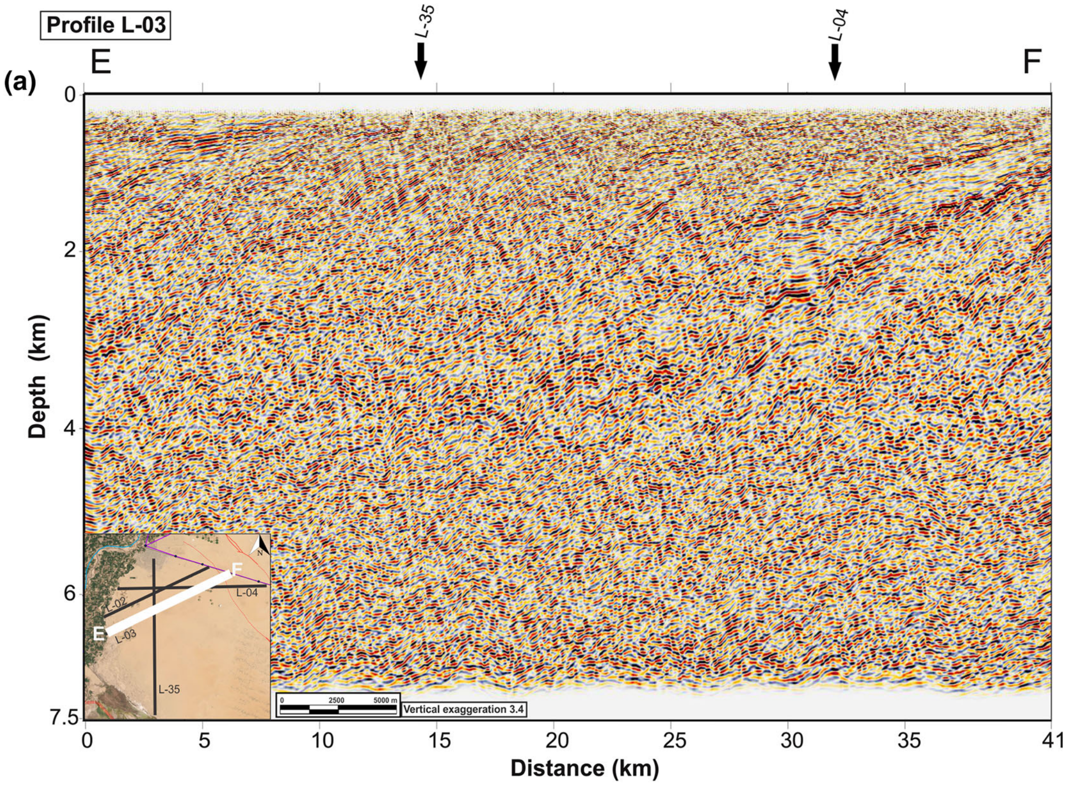
Profile L-03
E
F
L-35
L-04
(a)
Depth (km)
Distance (km)
Vertical exaggeration 3.4
0
2500
5000 m
L-02
L-03
L-04
L-35

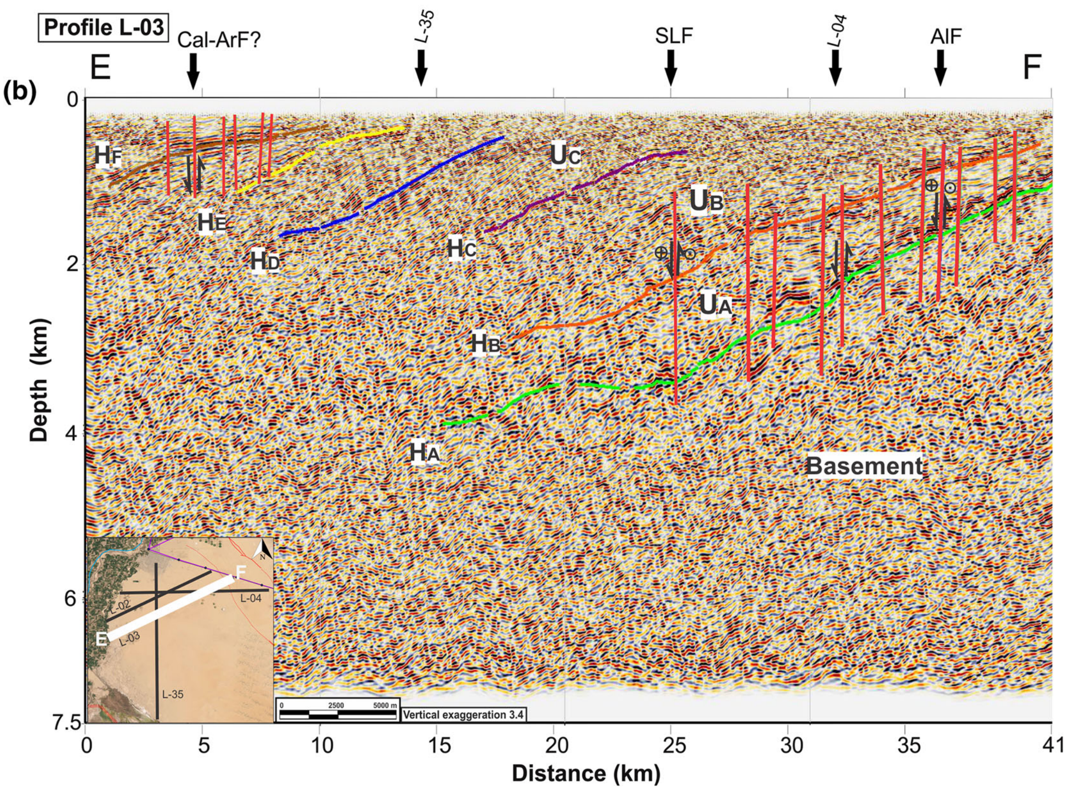
Profile L-03
Cal-ArF?
L-35
SLF
L-04
AlF
E
F
(b)
HF
HE
HD
HC
UC
UB
UA
HB
HA
Basement
Depth (km)
Distance (km)
Vertical exaggeration 3.4
0
2500
5000 m
L-02
L-03
L-04
L-35

◀Figure 5
Seismic line L-03, uninterpreted (**a**) and interpreted (**b**). Two of the three primary seismic reflectors are observed (HA and HB), while the HC is less clear (purple horizon). Shallow reflectors were identified (HD, HE, HF). The set of faults in the SW sector is the same observed in seismic line L-02 (Fig. 4). Red lines are faults. Arrows indicate relative apparent vertical motion. Circle-dot and circle with x indicate suspected strike-slip motion component. *SLF* San Luis fault. *AlF* Altar fault. *Cal-ArF* Calipatria-Arena fault. *H*—Horizon

line L-35. We interpret HA to correspond with the top of the acoustic basement, which was encountered at 2870 m by well W-1 (Fig. 3). The basement has a chaotic pattern of reflections beneath HA, which is a seismic reflector of high acoustic impedance. The top-of-basement surface has an apparent dip to the south in L-35, towards well W-4 ($\sim$ 5 km depth), but this well did not encounter basement. Thus, the basement, and the floor of the Altar basin, must have an apparent southward dip beneath the bottom of well W-4. Seismic line L-35 also shows sigmoidal clinoforms in Unit B, in an area where crystalline basement deepens to the south, which has been interpreted by Pacheco et al. (2006) as classic clinoform shapes related to the southward progradation of the Colorado River delta (Fig. 7). Seismic line L-05, taken for visualization from Reyes-Martinez et al. (2021). is 30 $\sim$ km north of the northern end of L-35 (see Figs. 2b and 7). L-05 is approximately perpendicular to L-35 and perpendicular to the southward advancement direction that Pacheco et al. (2006) interpreted for the arriving Colorado River delta. In contrast to L-35, seismic line L-05 shows hummocky clinoforms which consist of irregular discontinuous subparallel reflection segments and looks less like a classic delta, a pattern which is expected to be observed in a seismic line that transects across a delta system where the direction of progradation is perpendicular to the seismic line (i.e., in or out of the seismic line). The hummocky clinoforms display an apparent gentle dip to the west on L-05. These hummocky features in Unit B also have an apparent gentle dip to the west in L-04 (Fig. 6). The HA, HB and HC horizons also have apparent west dips on L-04. These three horizons have apparent dips to the southwest on L-02 and L-03, and to the south on L-35. Taken together, the observations from all five of these seismic lines suggest that the hummocky Colorado River sediments and their bounding horizons likely dip to the SW. This supports the idea that, although the Colorado River sediments may have been deposited in a southward prograding delta, these deposits appear to have experienced subsequent tilting to the SW.

Wells W-1 and W-4, and the seismic line L-35 in the region of the Altar basin are located outside of the modern area of the Colorado River delta (CRDA) (Fig. 1). However, these wells reported sediments from the Colorado River (Pacheco et al., 2006), suggesting that this river once had a presence in our study area. The network of distributary channels in the modern-day Colorado River is only observed in the Colorado River Delta Area (Fig. 1). Kinsland and Lock (2001) interpret a gravimetric low in the Altar basin region as a depression in the basement where the Colorado River could have been funneled following the NW–SE-oriented Altar basin (Fig. 2b).

Additional perspective on the geometry and architecture of the floor of the Altar basin comes from mapping the top-of-basement reflector (HA) on the other three seismic lines. On seismic line L-04 (Fig. 6), HA has an apparent dip to the west and is shallower at the east end of the line. The horizon that represents the top of acoustic basement (HA) presents strong amplitude, and no continuous (or coherent) reflections or structures are observed below it, similar to seismic line L-35. A local deformation zone is observed at the San Luis fault, between km 6 and km 14 at a depth of $\sim$ 5000 m, where the top of basement locally dips to the east on the eastern flank of a structural basement high. Seismic line L-02 shows the top of basement with an apparent dip to the southwest, except where the San Luis fault forms a local deformation zone with apparent southwest-side-up offset along the margin of the same structural basement high. The same basement behavior is shown in the seismic line L-03, as it is parallel and close to seismic line L-02. The apparent dip of the top of basement (HA) across seismic line L-02 is towards the southwest, except at a possible local structural high observed along the San Luis fault, between km 15 and km 20.

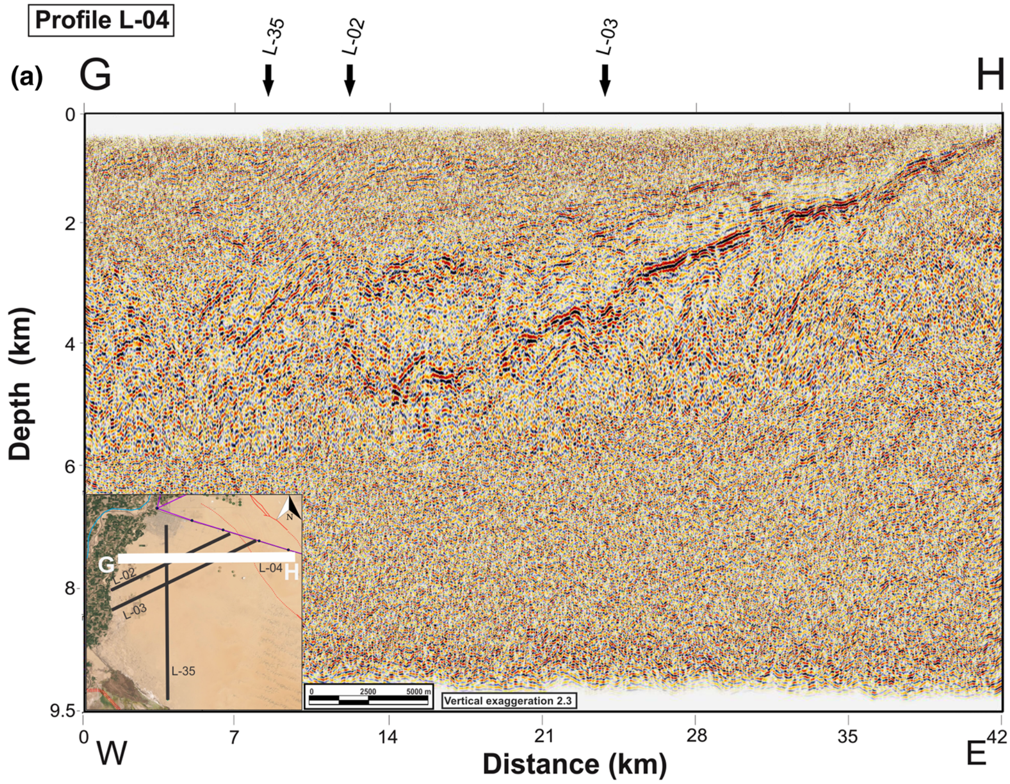
Profile L-04
(a)
G
H
L-35
L-02
L-03
Depth (km)
0
2
4
6
8
9.5
0
7
14
21
28
35
42
W
E
Distance (km)
L-02
L-03
L-04
L-35
Vertical exaggeration 2.3

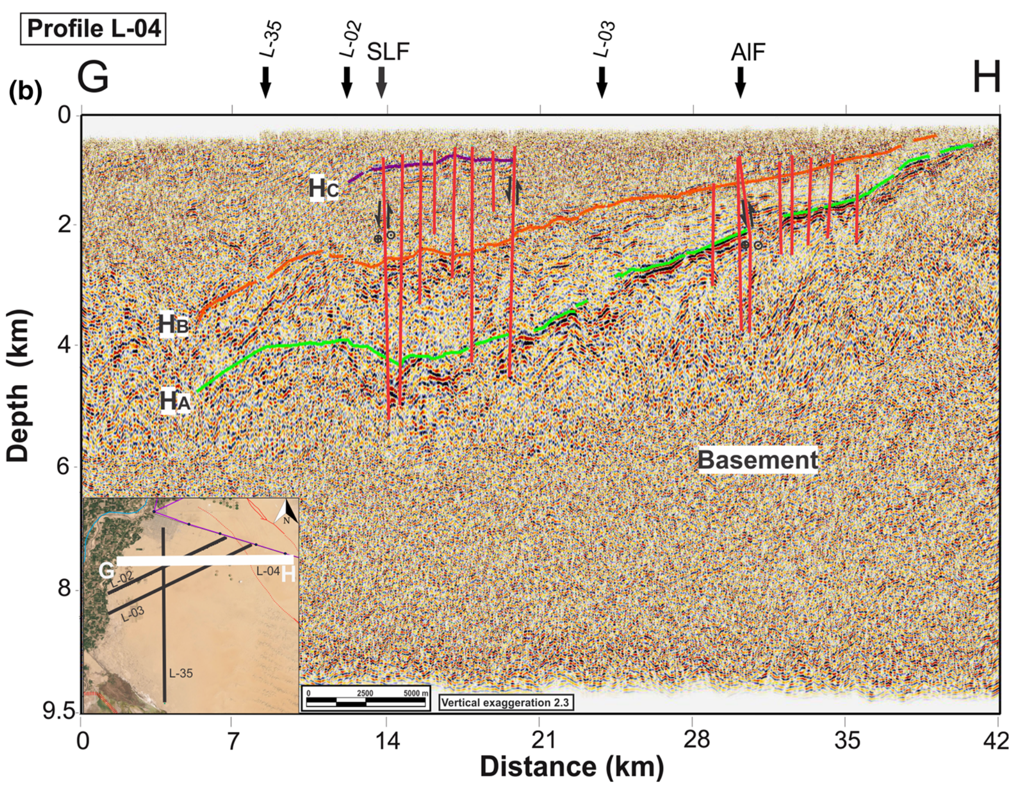
Profile L-04
(b)
G
H
L-35
L-02
SLF
L-03
AIF
HC
HB
HA
Basement
Depth (km)
0
2
4
6
8
9.5
0
7
14
21
28
35
42
Distance (km)
L-02
L-03
L-04
L-35
Vertical exaggeration 2.3

◀Figure 6
Seismic line L-04, uninterpreted (**a**) and interpreted (**b**). Three strong seismic reflectors are observed, including HA, which separates the basement from the mudstone Unit A. Overlying Unit A, HB is in orange, and HC is also visible in purple, being cut by a series of faults. Red lines are faults. Arrows indicate relative apparent vertical motion. Circle-dot and circle with x indicate suspected strike-slip motion component. *AlF*—Altar Fault; *SLF*—San Luis fault; *H*—Horizon

Finally, from the correlation of all interpreted seismic reflectors, and constraints from the drill holes, we created 3D irregular surface interpolations of all horizons (HA through HF) (Fig. 8). From this integrated dataset, we can visualize the southwest-dipping geometry of the floor of the Altar basin, which corresponds with the top of basement (HA) except where it is locally disrupted along a NW-trending basement high bounded on its eastern side by the San Luis fault (Fig. 8). Furthermore, all of the other younger horizons (HB, HC, HD, HE) also dip to the SW (Figs. 7, 8). Importantly, each younger horizon dips more gently than older horizons. Thus, this progressive up-section shallowing of dip might be evidence for syn-depositional SW tilting and basin subsidence. Additionally, all sedimentary units tend to shallow towards the NE and appear to be eroded and truncated near 0 km depth as seen in seismic lines L-02 and L-03 (Figs. 4, 5). These units do not appear to thin dramatically towards the NE, supporting the idea that the block between the Altar fault and the Cerro Prieto fault might have experienced tilting down-to-the-SW. We used a gravity anomaly map, located relative to our surface interpolations, as an auxiliary tool for the interpretation, since it indicates the lower and higher density zones that help to identify structural highs and lows (Figs. 2a, 8), such as in the east of the study area, where a gravity high is observed between the Altar fault and Rosario fault and collocated with the Sierra El Rosario (Fig. 9).We used the magnetic anomaly map which shows the size and locations of magnetic anomalies related to different structures in the region, such as a large NW–SE-oriented low magnetic anomaly in the Altar basin that we interpret to represent the sedimentary basin fill of the Altar basin, a huge elongated sedimentary basin which continues to the southeast in the Bahia de Adair region (Fig. 2).

4. Discussion

From the interpretation of the seismic lines, we confirm the existence of several faults, most of them buried by relatively younger, unfaulted sediments. Only thirteen faults can be correlated across two or more seismic lines (Fig. 9), including the Altar fault, previously reported at the NE edge of the Altar basin by Pacheco et al. (2006) and González-Escobar et al. (2013). We document several additional faults in the four seismic lines analyzed in this study, which could not be correlated in two or more seismic lines.

4.1. Altar-Dunas Fault

We identified the Altar fault in two seismic lines. First, in seismic line L-04, the Altar fault produces significant apparent down-to-the-west vertical offset of ~ 450 m of the top of basement (Fig. 6b). Second, the Altar fault is also present in seismic line L-03, where we estimate ~ 250 m apparent down-to-the-southwest vertical offset of the top of basement (Fig. 5b). The Altar fault has an apparent dip to the SW reported from seismic reflection studies southwest of our study area (Gonzalez-Escobar et al., 2013), while in our seismic lines it has apparent dip to the west in seismic line L-04 and to the southwest in seismic line L-03. Possible evidence of movement of this fault is the poor correlation in the reflectors nearby, due to very diffuse reflections, which may represent areas of fault-related rock damage. Based on the correlation of the Altar fault, in these two seismic lines, the fault strikes NW. This NW trend is aligned with the Dunas fault, a NW-striking fault located along-strike to the northwest, with similar down-to-the-SW fault motion (Reyes-Martinez et al., 2021). So, we speculate that the Altar fault and Dunas fault could be the same continuous structure (Figs. 8, 10). Note that the Altar fault was not observed on seismic line L-02 because the fault is likely located beyond and northeast of the end of this seismic line.

4.2. San Luis Fault

The San Luis fault produces a deformation zone observed in three of the seismic lines (L-02, L-03, L-04) affecting both HA (top of basement) and HB. We interpret the San Luis fault to have an apparent dip to the SW. The San Luis fault bounds the northeast side of a possible structural high, however, its geometry was not well defined due to the poor resolution. Furthermore, a set of four NW-striking, subvertical faults was observed sub-parallel to the San Luis fault, spaced less than 1 km apart, correlated in seismic lines L-02 and L-03 (Figs. 9, 10).

4.3. Calipatria-Arena Fault System

A set of six faults spaced apart by less than 1 km was interpreted and correlated in two seismic lines (L-02 and L-03). These faults have a NW–SE orientation and have an apparent dip to the southwest, and are located above a gravity high in the anomaly map (Fig. 9). These northwest-striking faults are

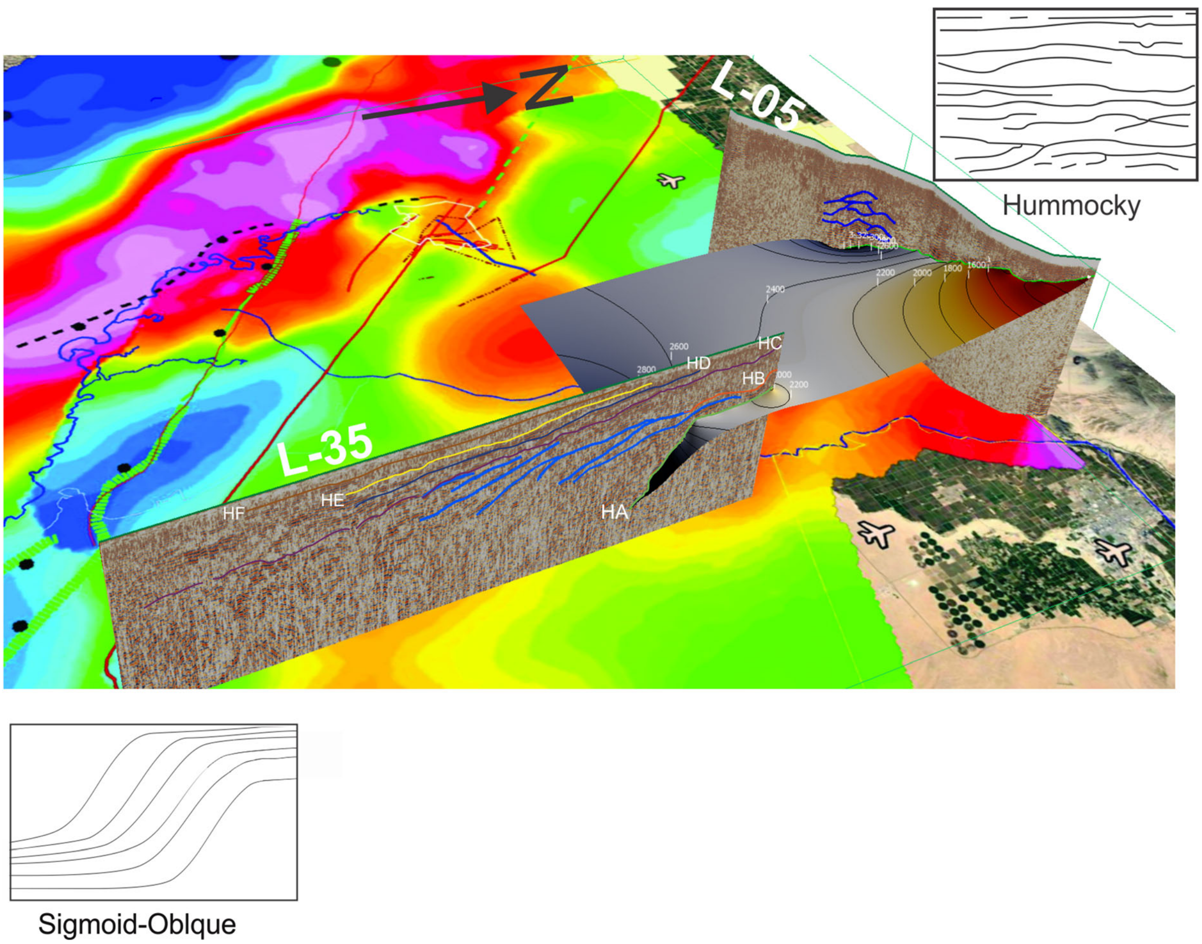

Figure 7
Oblique view to the northwest of seismic line L-35 and L-05 in the northern portion of the Altar basin. Seismic line L-35 shows sigmoidal-oblique clinoforms, and seismic line L-05 shows hummocky-type clinoforms, a pattern which is expected to be observed in a seismic line that transects a delta system where the direction of progradation is perpendicular to the seismic line (i.e., in or out of the seismic line). Seismic line L-35 shows the classic clinoform shapes, while seismic line L-05, which is perpendicular to L-35, shows a perpendicular view to the clinoform shapes and looks less like a classic delta

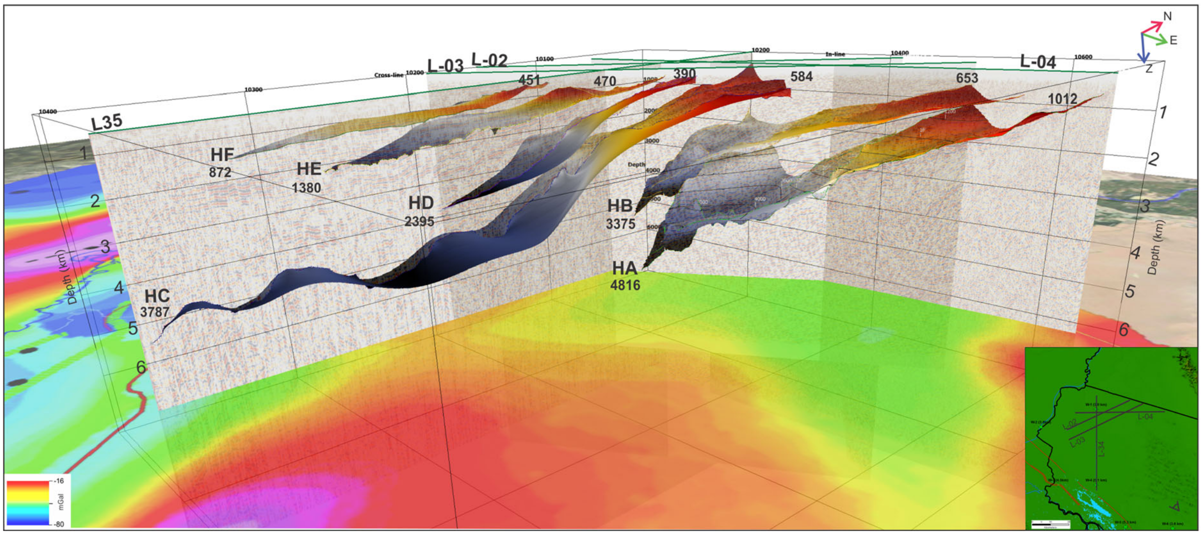

Figure 8
Oblique view towards the northwest of 3D surface interpolations of all interpreted seismic reflectors, located relative to the Bouguer gravity anomaly map. All 6 seismic horizons dips to the southwest and horizons have a semi-parallel behavior between them. As it gets deeper, acoustic basement surface (HA) shows a more irregular behavior than the other horizons. The younger horizons (HD, HE, HF) are more gently inclined than the older, deeper horizons (HA, HB, HC), which could be an indicator of cessation of activity in the basin. Numbers at the ends of each horizon indicate maximum and minimum depth in meters

collinear with the Calipatria fault reported by Fonseca et al. (1981), and they are also collinear with the Arena fault, along-strike to the southeast (Fig. 9). More detailed studies are needed to be able to correlate this set of faults with the Arena fault, since they do not share the same sense of motion with the Arena fault in seismic line L-35 (Fig. 3). However, the Arena fault in seismic line L-35 is over a local gravimetric high, that could be related to its change in the sense of vertical fault motion, since intrusive units have been reported NW of the study area (Reyes-Martinez et al., 2021). Although it was not possible to know if these structures had surface expression due to the low resolution of the seismic data, the RESNOM (Red Sísmica del Noroeste de México) catalog has not registered any seismic activity in the area where these faults are located, which could mean that they are not tectonically active. These faults are observed at depths between 250 and 1800 m and appear to cut Units UE and UF (Figs. 9, 10).

4.4. Rosario-Algodones Fault

The Rosario fault (Gonzalez-Escobar et al., 2013), is a NW-striking, NE-dipping fault located to the east of the Sierra El Rosario (Figs. 1 and 2a). The Algodones fault is mapped along-strike to the northwest as a normal fault, where the land surface southwest of the fault is 30–60 ft higher than the surface to the northeast (Olmsted et al., 1973), so this fault is interpreted to dip to the NE, and is parallel to the San Andreas fault system (Fig. 1). Neither the Rosario nor Algodones faults were observed in this study because they are located east of the four seismic lines examined here. We propose that the Rosario fault and the Algodones fault are the same continuous NE-dipping structure because they are collinear and their traces are both located east of the Sierra El Rosario (Fig. 9).

4.5. Detachment Fault

The southeast edge of the Altar basin is bounded by a detachment-type fault with a northwest dip as reported by Pacheco et al. (2006) (Fig. 11), who postulated that this detachment fault was active

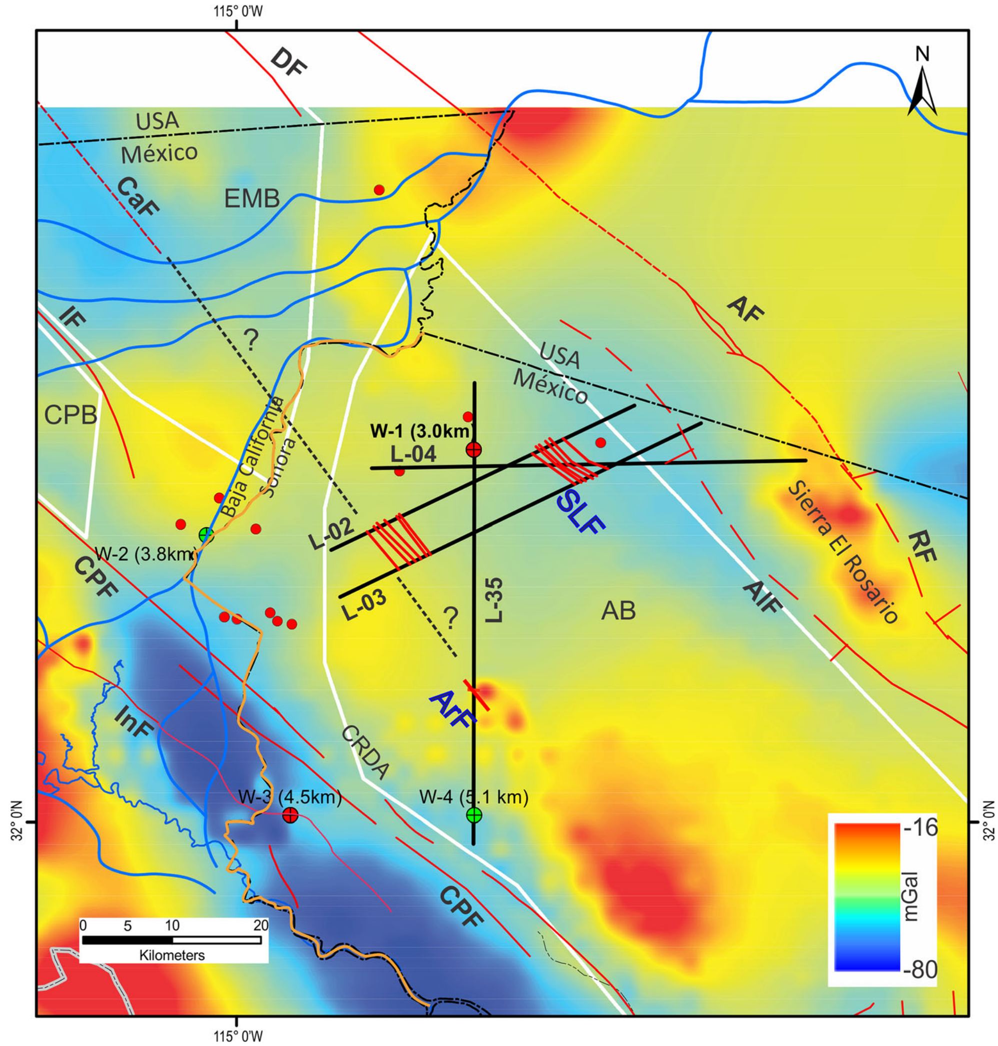

Figure 9

Faults interpreted in this study (short red lines) over the Bouguer anomaly map. Black straight lines—seismic lines. Red lines—faults. Wells in México that penetrated and did not penetrate basement are red and green circles with black crosses, respectively, with numbers indicating its depth. Red circles—Hydrothermal surface manifestations (Arango-Galván et al., 2015). White polygons—sedimentary basins: *EMB*—East Mesa basin, *CPB*—Cerro Prieto basin, and *AB*—Altar basin. *ArF*—Arena fault; *SLF*—San Luis fault; *DF*—Dunas fault; *CaF*—Calipatria fault; *IF*—Imperial fault; *CPF*—Cerro Prieto fault; *InF*—Indiviso fault; *AlF*—Altar fault; *RF*—Rosario fault; *AF*—Algodones fault

during deposition of Units A and B. The marine sequence (A) overlying the crystalline basement is interpreted as having experienced tectonic transport along the northwest dipping fault. Pacheco et al. (2006) suggest that the Altar fault and this detachment fault may have been linked to the transtensional domain of the southern San Andreas Fault system during the late Miocene and Pliocene. Bennett et al. (2017) highlights how, during late Miocene time, faults bounding the Altar basin, such as the Altar fault, were likely kinematically linked to the eastern California shear zone farther northwest and to the Gulf of California shear zone farther southeast. This detachment fault was likely an important structure controlling the formation of the Altar pull-apart basin related to this late Miocene transtensional activity.

We reexamined two seismic lines (5013 and 5024prol) reported by González-Escobar et al. (2013)

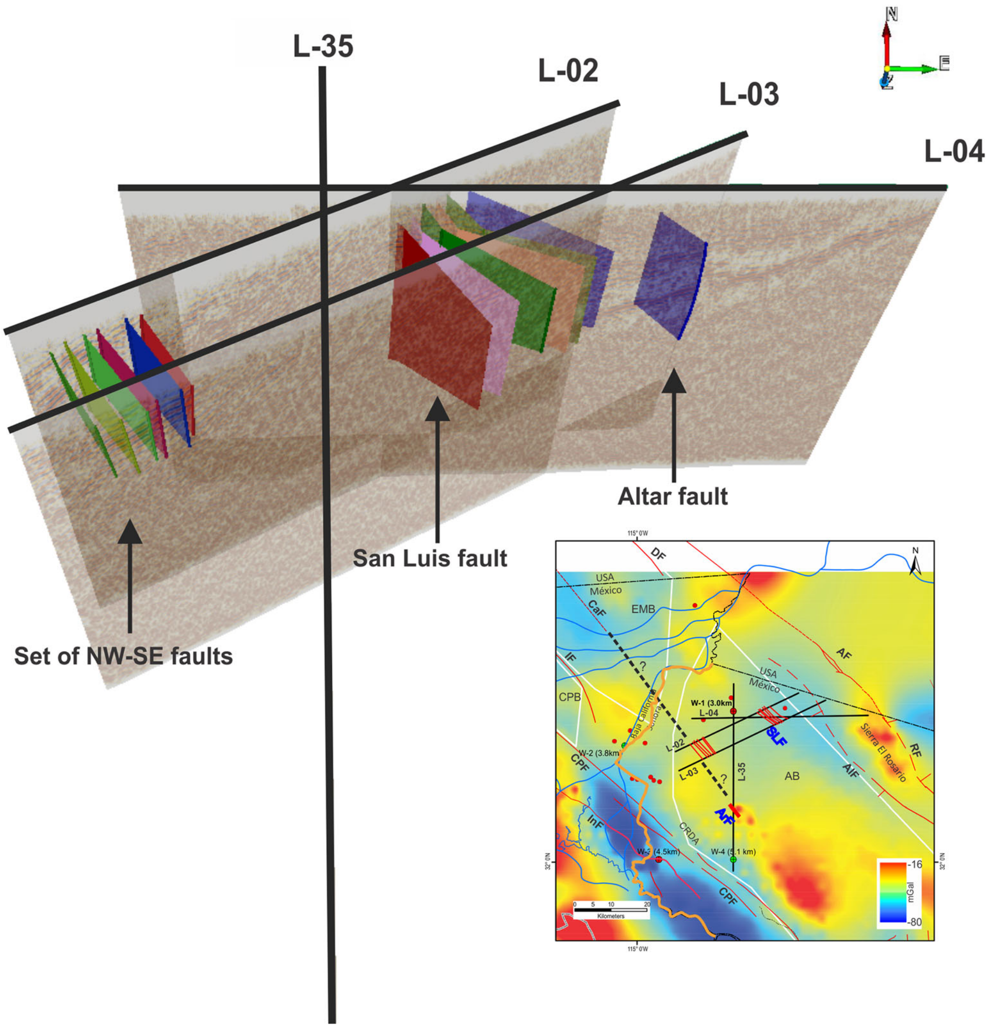

Figure 10
Steep oblique view to the north, showing seismic lines analyzed in this study and planar fault surfaces interpreted correlated across seismic lines. These short faults are shown as short red lines on the inset map (and Fig. 9)

in the area where the detachment fault has been mapped. In this area, the Kahwan fault (KaF) is observed in both seismic line 5013 and seismic line 5024prol (Fig. 11). The Torres detachment fault (TF) is observed in seismic lines 5034a, 5003, and 5005.

Considering that UA overlies the crystalline basement, and HA is the top of acoustic basement, according to Pacheco et al. (2006), the top of the acoustic basement is not only the basal contact of UA but is also the fault plane of the proposed detachment (Fig. 11A, B and D, in yellow), suggesting that UA is locally in fault contact with basement rocks. However, from our reexamination of these two seismic lines (Fig. 11A, B, and D), we interpret the contact between UA and acoustic basement as a depositional contact, and not a fault, because we do not see that detachment fault (Fig. 11A, B, D in yellow) in seismic lines 5024prol and 5013, which is where Pacheco et al. (2006) propose its existence. There is no evidence of drag folds, or secondary faults connecting to the proposed low-angle fault (Fig. 11D). Also, the seismic horizons that we interpret as sediments, are semi-parallel to the acoustic basement, and are not cut by the proposed

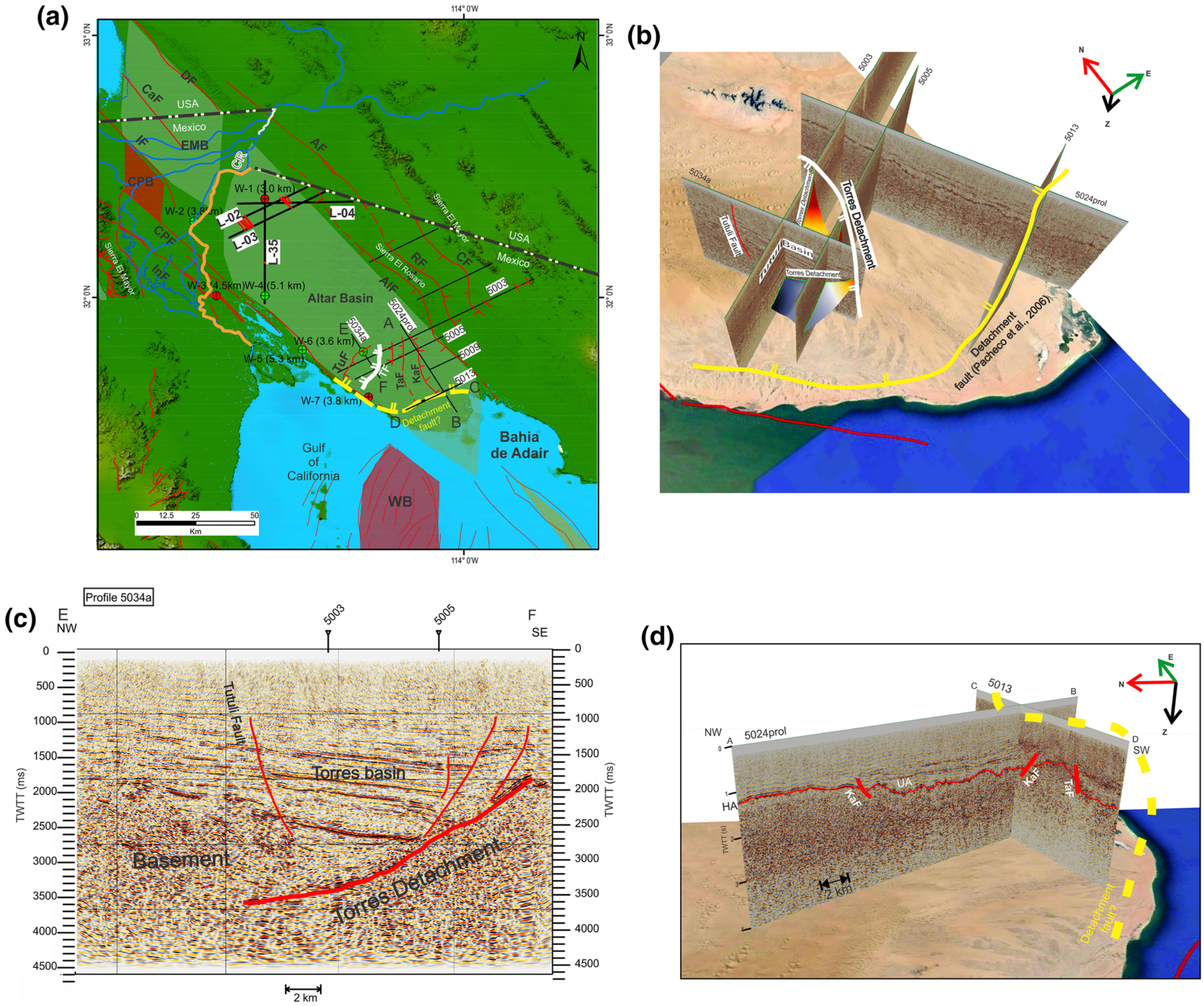

Figure 11

a Map focused on the detachment fault proposed (yellow line) by Pacheco et al., (2006) and seismic lines 5003, 5005, 5024prol, 5034a, and 5013 (black lines) from González-Escobar et al., (2013), reexamined in this study. *EMB*—East Mesa basin, *CPB*—Cerro Prieto basin, and *WB*—Wagner basin. Faults in red color: *DF*—Dunas fault; *CaF*—Calipatria fault; *IF*—Imperial fault; *CPF*—Cerro Prieto fault; *InF*—Indiviso fault; *AlF*—Altar fault; *RF*—Rosario fault; *AF*—Algodones fault; *CF*—Caborca fault; *TuF*—Tutuli fault; *TF*—Torres fault; *TaF*—Taracahita fault; *KaF*—Kahwan fault. **b** Oblique view to the northeast, showing projection of the Torres fault plane with the seismic lines that intersect it, including the detachment fault reported by Pacheco et al. (2006) in yellow. **c** Seismic line 5034a show the Torres detachment fault and Torres basin. **d** Oblique view to the southeast, showing the projection of two of the seismic lines in the area where the detachment fault reported by Pacheco et al. (2006) is projected and where its presence is not observed within the resolution of the seismic lines

fault (Fig. 11D). Also, this seismic reflector is not as smooth as other reported detachment faults (i.e. Cañada David detachment, González-Escobar, 2016). From this, it is difficult to visualize the presence of a detachment fault in that region. This does not imply that the detachment fault is not present to the north, south or deeper than the sector observed in this work. On the other hand, many of the characteristics previously mentioned are visible in the Torres detachment fault in seismic line 5034a (Fig. 11C) such as a drag fold, and a smooth fault plane slightly tilted with subsidiary faults connecting with the Torres detachment fault. Also, we see a basin which we called Torres basin, bounded by the Tutuli fault and Torres fault (Fig. 11C).

4.6. Tectonic Implications

Deformation in the Gulf of California shear zone involves an evolution of active fault-controlled pull-apart basins shifting towards the west with time, which has produced abandoned late Miocene transtensional basins along the eastern margin of the Gulf of California (Aragón-Arreola and Martín-Barajas, 2007a, b; Bennett & Oskin, 2014), such as the Altar basin (Pacheco et al., 2006; this study), the Tecomate basin on northeast Isla Tiburón (Bennett et al., 2017), and the Punta Chueca and Kino basins in coastal Sonora (Bennett et al., 2013). The abandonment of the Altar basin likely resulted from the relocation of plate boundary deformation from the Altar fault onto the Cerro Prieto fault (Fig. 1). Seismic line L-35 shows the Arena fault, a significant fault that affects the three seismostratigraphic units (A, B, and C) identified by Pacheco et al. (2006), and identified in this work (UA, UB and UC). However, this fault has a minimal impact on two shallower horizons (HE and HF), which have great lateral continuity and have a large distribution along the seismic line, contrary to older horizons HA, HB and HC that have steeper dips. The Altar and San Luis faults display a similar behavior, where Unit C is the youngest unit cut by these faults. However, the younger units (D, E, and F) are not mapped above the Altar and San Luis faults (Figs. 5 and 6), thus, the end of fault activity on these structures is less well constrained. The history of motion on the Arena fault could be an indicator of abandonment of the activity in the basin, recording the westward shift of the Pacific-North America plate boundary from the Altar basin to basins west of the Cerro Prieto fault.

4.7. Bouse Formation

Upon comparison of seismic line L-04 with borehole observations and cross sections (Olmsted & McDonald, 1967; Olmsted et al., 1973) along the US-Mexico border, we interpret that Unit A correlates to the basal carbonate member of the Bouse Formation (Figs. 1, 12). Unit B, which is a transition zone of alluvium and marine sedimentary rocks, might be the siliciclastic member of the Bouse Formation. While Unit C, is characterized by a substantial increase in the proportion of sand relative to mud and silt. Sand intervals are progressively thicker and include conglomerate deposits and subordinated mud-silt strata in wells reported by Pacheco et al. (2006). We consider Unit C might correlate to Bullhead Alluvium; however more detailed studies are required in this area. Olmsted et al. (1973) reported the presence of Bouse Formation in the subsurface in the region of Yuma, AZ (Fig. 12a) along the US-México border, less than 10 km from the seismic lines examined in this work. On seismic line L-04, we interpreted UA to be in nonconformable depositional contact above basement, with the top of the Bouse Formation (HB) varying from slightly greater than 1 km ($\sim$ 3300') deep immediately west of the Altar fault to $\sim$ 2.5 km ($\sim$ 8200') deep near the San Luis fault (Figs. 6 and 12). Such an interpretation is consistent with the depth at which this formation is reported in the northern part of the Altar basin, just north of the US-Mexico border, where Olmsted and McDonald (1967) and Olmsted et al. (1973) speculated that the top of Bouse Formation varies from 2500 to 3000' ($\sim$ 0.75 to 1 km) deep west of the Altar fault and deepens towards the southwest (Fig. 12). Pacheco et al. (2006) report from well data that Unit A is from late Miocene to early Pliocene marine sedimentation, which shows distinctive parallel, low-amplitude, discontinuous reflectors, and a widespread distribution in the northern Altar basin. The correlation of Unit A with the basal carbonate member of the Bouse Formation is also supported by the age assigned to the latter, of $\sim$ 6.1 to 5.3 Ma (McDougall and Miranda-Martinez, 2014; Miranda-Martinez et al., 2017).

To evaluate our proposed correlation of Unit A with the basal carbonate member of the Bouse Formation and to see the distribution of this unit in the northern Altar basin, we combined the depth contours of the top of the Bouse Formation in southwestern Arizona (Olmsted et al., 1973) with depth to the top of Unit A (horizon B; HB) from our seismic line interpretations in northwestern Sonora (Fig. 12b). The results illustrate how this unit deepens to the southwest reaching depths of about 3800 m. We were unable to confidently map the Bouse Formation farther southwest towards the Cerro

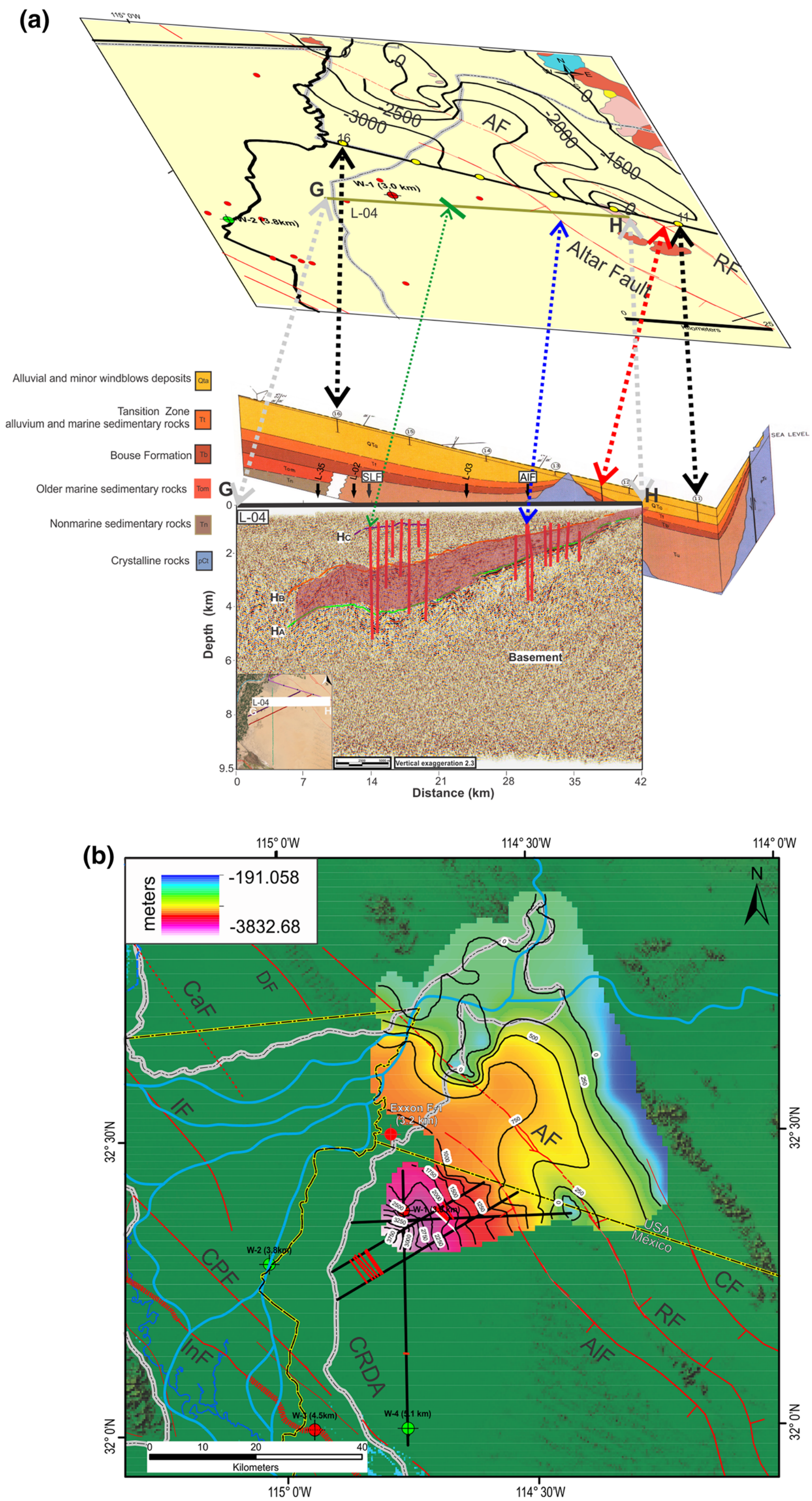
(a)
AF
Altar Fault
RF
G
H
L-04
W-1 (3.0 km)
W-2 (3.8km)
Alluvial and minor windblows deposits
Tansition Zone alluvium and marine sedimentary rocks
Bouse Formation
Older marine sedimentary rocks
Nonmarine sedimentary rocks
Crystalline rocks
SEA LEVEL
SLF
AlF
Basement
Depth (km)
Distance (km)
Vertical exaggeration 2.3
(b)
meters
-191.058
-3832.68
115° 0'W
114° 30'W
114° 0'W
32° 30'N
32° 0'N
CaF
DF
IF
CPF
InF
CRDA
AF
RF
AlF
CF
USA
Mexico
Exxon E-1 (3.2 km)
W-2 (3.8km)
W-3 (4.5km)
W-4 (5.1 km)
Kilometers

Figure 12
a Oblique view to the north-northeast, showing the subsurface geometry of the northern Altar basin near Yuma, CA. Geological cross section (along the USA-Mexico international border) and explanation (hanging in subsurface). Contour lines (on map) indicating depth in feet of the top of the Bouse Formation (Olmsted et al., 1973). Table 1 lists the depths (feet) of wells in Arizona and California. Seismic line L-04 shown in foreground for comparison of relationships to the geologic cross section. Locations on the map are tied to their locations on the geologic cross section and seismic line L-04 with dashed lines. We correlate Unit A on seismic line L-04 with the Bouse Formation (Tb) on the geologic cross section. The three main seismic horizons (HA, HB, HC) are the basal contacts of sedimentary sequences A, B, and C. HA separates the top of basement from the overlying mudstone Unit A. Overlying Unit A, HB is in orange and, the HC is visible in purple (Pacheco et al., 2006). Red lines indicate the interpreted faults. *AlF*—Altar fault; *SLF*—San Luis fault; *H*—Horizon; *U*—Unit. **b** Surface contour correlation between depths of the top of the Bouse Formation reported by Olmsted et al., (1973) and depths of HB interpreted in this work. This compilation illustrates how the Bouse Formation southwest of the Altar fault deepens to the southwest over a very short distance, reaching depths greater than 3800 m

Prieto fault due to poor quality seismic data below ~ 4–5 km depths, where this unit appears to continue to greater depths towards the southwest. However, one distinction between seismic line L-04 and the well data and cross sections from earlier studies (Olmsted et al., 1973) is the presence of older marine sedimentary rocks and nonmarine sedimentary rocks beneath the Bouse Formation, which we do not see in the seismic lines that we analyzed. Nevertheless, we cannot rule out the possibility that these sequences exist in the northern part of the Altar basin in northwestern Sonora. Furthermore, autochthonous benthic foraminifera and autochthonous ostracods were reported at the very top of Unit A in Well-1 (Helenes et al., 2009; Pacheco et al., 2006). Although detailed studies are needed to find more evidence on the presence of any of the members of the Bouse Formation in our study area, the same fauna has been reported for the Bouse Formation in the Yuma area (Olmsted et al., 1973), supporting the interpretation that Unit A in the Altar basin is the basal carbonate member of the Bouse Formation and, thus, provides new evidence that the Bouse Formation extends in the subsurface into NW Mexico.

5. Conclusions

(1) The 3D subsurface architecture of the Altar basin, interpreted from mapping the top of acoustic basement, indicates that the basin deepens to the southwest, and it might have formed a structural trough, oriented NW–SE, into which the Colorado River could have been funneled (Fig. 2a, b, 7). Basement rocks beneath the Altar basin shallow towards the NE where they emerge in the Sierra El Rosario, which is consistent with the patterns from previous gravity and magnetic maps.

(2) The Altar fault in the northeastern region of the Altar basin is observed in two seismic lines, with an orientation of N45°W, with a down-to-the-southwest vertical offset of ~ 450 to ~ 250 m on the top of basement. This fault is colinear with the NW-striking Dunas fault in southeastern California and may be the same structure. The Altar fault and the detachment fault (Pacheco et al., 2006) may have been linked to the transtensional domain of the southernmost San Andreas fault in the late Miocene to Pliocene.

(3) The Algodones and Rosario faults are likely the same structure, located along the northeastern margin of the Sierra El Rosario. The Algodones-Rosario fault system is parallel to the Altar fault, but dips in the opposite direction to the northeast. Together the Altar-Dunas and Algodones-Rosario fault systems form the structural margins of a NW-oriented horst block.

(4) The San Luis fault, reported here for the first time, is a NW-striking fault that defines the northeastern margin of a structural high in the center of the Altar basin. The San Luis fault affects the top of the acoustic basement and Unit A at the base of the basin. Above this, Units B and C are semi-horizontal and cover the structural high, suggesting that this structure was active until late Miocene to early Pliocene time, when Unit A was deposited (Pacheco et al., 2006).

(5) A set of NW-striking faults are subparallel to the San Luis fault; these faults are separated less than 1 km from each other. Also, several NW-striking faults were identified in the shallow subsurface of

seismic lines L-03 and L-02, colinear to the Arena Fault and Calipatria fault, between depths of 250 and 1800 m; however, the RESNOM catalog has not registered seismic activity in the area, so it is not known if they are tectonically active. Alternatively, these would be small faults that accommodate recent basin subsidence by compaction of the sedimentary sequence.

(6) Altar basin sedimentary deposits above horizon C are less affected by the faults in seismic line L-35. In contrast, horizons A, B and C are cut by faults and have a greater dip and less lateral continuity in the same line. The Arena fault is a significant fault that affects the three seismostratigraphic units UA, UB and UC, but has a minimal impact on two shallower units (UE and UF), allowing these younger units to have greater lateral continuity and a larger distribution on the seismic line. This behavior is also seen with the Altar fault and San Luis fault, where Unit C is the youngest unit cut by these structures. We suggest that this could be an indicator of the abandonment of the Altar basin in Pliocene–Pleistocene time.

(7) We propose that Unit A in the Altar basin may correlate with the Bouse Formation defined in the Yuma, AZ area, based on the comparison and correlation of previously-reported seismic lines and drill holes (Olmsted et al., 1973). Also, Unit A in the Altar basin and the subsurface Bouse Formation near Yuma contain similar fauna (benthic foraminifera and ostracods).

(8) It was not possible for us to identify features that could support the theory that a NW-dipping detachment fault is controlling subsidence of the Altar basin in the area where it was proposed (Pacheco et al., 2006). However, we cannot rule out the possibility that this detachment fault exists to the north or south, or exists deeper and below the bottom of these seismic lines. Faults within and along the margins of the Altar basin appear to have initiated during late-Miocene time and were likely active until Pliocene–Pleistocene time. Additionally, it was possible to find SW tilting of sedimentary units, and younger horizons dipping more gently than the older horizons, which might suggest syn-depositional SW tilting and basin subsidence.

(9) We interpreted that the Altar fault represents the eastern margin of the Altar pull-apart basin. The Altar basin and the faults that controlled basin formation are likely components of the late Miocene to Pliocene Pacific-North America plate boundary, linking transtensional structures of the eastern California shear zone in the lower Colorado River region to the northwest (e.g., Dorsey et al., 2017, 2021a, b) with transtensional structures of the Gulf of California shear zone to the southeast (e.g. Bennett & Oskin, 2014; Bennett et al., 2017). Basin activity was abandoned in the Pliocene as fault-related basin subsidence migrated towards the west into the Cerro Prieto and Laguna Salada basins.

Acknowledgements

We are indebted to CONACYT, Mexico, for financial support through scholarships; to PEMEX Exploración y Producción for allowing the use of seismic data and to Halliburton/Landmark software and OpendTect for the use of their software through the University Grant Programmes to CICESE, Baja California, Mexico. We thank Scott E. K. Bennett and an anonymous reviewer whose comments/suggestions helped improve and clarify this manuscript. J. Stock was supported by US National Science Foundation grant EAR-1728690.

Author Contributions All authors contributed to the study conception and design. Material preparation, data processing and analysis were performed by JP, and MG. The first draft of the manuscript was written by JP, and all authors commented on previous versions of the manuscript. All authors read and approved the final manuscript.

Funding

We are indebted to CONACYT, Mexico, for financial support through a Master's scholarship. J. Stock was supported by US National Science Foundation grant EAR-1728690.

Declarations

Conflict of interest The authors have no relevant financial or non-financial interests to disclose.

Publisher's Note Springer Nature remains neutral with regard to jurisdictional claims in published maps and institutional affiliations.

References

Aragón-Arreola, M. & Martín-Barajas, A. (2007a). Acomodo de la Deformación en el Norte del Golfo de California, dentro del Margen Transtensivo entre las Placas Pacifico y NorteAmérica: *IX Congreso Geológico Venezolano*, 12 p.

Aragón-Arreola, M., & Martín-Barajas, A. (2007b). Westward migration of extension in the northern Gulf of California, Mexico. *Geology*, 35:571-574

Arango-Galván, C., Prol-Ledesma, R. M., & Torres-Vera, M. A. (2015). Geothermal prospects in the Baja California Peninsula. *Geothermics, 55*, 39–57.

Bennett, S. E., & Oskin, M. E. (2014). Oblique rifting ruptures continents: Example from the Gulf of California shear zone. *Geology, 42*(3), 215–218.

Bennett, S. E., Oskin, M. E., & Iriondo, A. (2013). Transtensional rifting in the proto-Gulf of California near Bahia Kino, Sonora, Mexico. *Bulletin, 125*(11–12), 1752–1782.

Bennett, S. E., Oskin, M. E., & Iriondo, A. (2017). Latest Miocene transtensional rifting of northeast Isla Tiburón, eastern margin of the Gulf of California. *Tectonophysics, 719*, 86–106.

Bright, J., Cohen, A. S., & Starratt, S. W. (2018). Distinguishing brackish lacustrine from brackish marine deposits in the stratigraphic record: A case study from the late Miocene and early Pliocene Bouse Formation Arizona and California, USA. *Earth-Science Reviews, 185*, 974–1003.

Chanes-Martínez, J. J., González-Escobar, M., Suárez-Vidal, F., & Gallardo-Mata, C. G. (2014). Structural geometry of a sector of the Colorado River delta, Baja California, Mexico, based on seismic reflections. *Pure and Applied Geophysics, 171*, 1107–1127. https://doi.org/10.1007/s00024-013-0729-z

Darin, M. H., Dorsey, R. J., Bennett, S. E. K., Oskin, M. E., & Iriondo, A. (2016). Late Miocene Extension in Coastal Sonora, México: Implications for the evolution of dextral shear in the proto-Gulf of California oblique rift. *Tectonophysics, 693*, 378–408. https://doi.org/10.1016/j.tecto.2016.04.038

Dibblee, T. W. (1984). Stratigraphy and tectonics of the San Felipe Hills, Borrego Badlands, Superstition Hills, and Vicinity. In A. C. Rigsby (Ed.), *The imperial basin; tectonics, sedimentation, and thermal aspects* (Vol. 40, pp. 45–70). Society of Economic Paleotologists and Minerologists Pacific Section.

Dorsey, R. J., Braga, J. C., Gardnerm, K., McDougall, K., & O'Connel, B. (2021b). *Early Pliocene marine transgression into the lower Colorado River valley, southwestern USA, by re-flooding of a former tidal strait* (p. 523). Geological Society.

Dorsey, R. J., O'Connell, B., Homan, M., & Bennett, S. E. (2017). Influence of the Eastern California Shear Zone on deposition of the Mio-Pliocene Bouse Formation: Insights from the Cibola area, Arizona. *Desert Symposium Field Guide and Proceedings. California State University Desert Studies Center, Zzyzx, CA*, p. 150–157.

Dorsey, R. J., O'Connell, B., McDougall, K., & Homan, M. B. (2018). Punctuated sediment discharge during early Pliocene birth of the Colorado River: Evidence from regional stratigraphy, sedimentology, and paleontology. *Sedimentary Geology, 363*, 1–33. https://doi.org/10.1016/j.sedgeo.2017.09.018

Dorsey, R. J., O'Connell, B., Gardner, K. K., Homan, M. B., Bennett, S. E., Thacker, J. O., & Darin, M. H. (2021a). Tectonostratigraphic record of late Miocene-early Pliocene transtensional faulting in the Eastern California shear zone, southwestern USA. *Geosphere, 17*(4), 1101–1125.

Espinosa-Cardeña, J. M., & Elders, W. A. (2003). Tectonic implications of gravity anomalies in the Northern Gulf of California and Salton Trough rift systems, in Cordilleran Section Meeting: Puerto Vallarta Mexico. *Geological Society of America, 35*, 26.

Fonseca L, H. L., de la Pena L, A., Puente C, I., & Diaz C, E. (1981) Extension of the Cerro Prieto field and zones in the Mexicali Valley with geothermal possibilities in the future (No. LBL-11967; CONF-810399-28). *Comisión Federal de Electricidad*, Mexicali, Mexico.

Gardner, K., & Dorsey, R. J. (2021). Mixed carbonate-siliciclastic sedimentation at the margin of a late Miocene tidal strait, lower Colorado River Valley, south-western USA. *Sedimentology, 68*(5), 1893–1922.

González-Escobar, M., Gallardo-Mata, C. G., Martín, A., Munguia, L., & Suárez-Vidal, F. (2016). Subsurface constraints of an active detachment fault in Laguna Salada basin, Baja California, México, from Interpretation of Seismic-Reflection Profiles. *Geosphere, 12*(4), 1283–1299. https://doi.org/10.1130/GES01261.1

González-Escobar, M., Mares Agüero, M. A., & Martin, A. (2020). Subsurface structure revealed by seismic reflection images to the southwest of the Cerro Prieto pull-apart basin, Baja California. *Geothermics, 85*, 1011779.

González-Escobar, M., Pérez-Tinajero, C. I., Suarez-Vidal, F., & González-Fernández, A. (2013). Structural characteristics of the Altar basin, Northwest Sonora, Mexico. *International Geology Review, 55*, 322–336. https://doi.org/10.1080/00206814.2012.708981

González-León, C. M., Valencia, V. A., López-Martínez, M., Bellon, H., Valencia-Moreno, M., & Calmus, T. (2010). Arizpe sub-basin: A sedimentary and volcanic record of Basin and Range extension in north-central Sonora Mexico. *Revista Mexicana De Ciencias Geológicas, 27*(2), 292–312.

Helenes, J., Carreño, A. L., & Carrillo, R. M. (2009). Middle to late Miocene chronostratigraphy and development of the northern Gulf of California. *Marine Micropaleontology, 72*, 10–25.

Henry, C. D., & Aranda-Gomez, J. J. (1992). The real southern basin and range: Mid- to late Cenozoic extension in Mexico. *Geology, 20*, 701.

Howard, K. A., House, P. K., Dorsey, R. J., & Pearthree, P. A. (2015). River-evolution and tectonic implications of a major Pliocene aggradation on the lower Colorado River: The Bullhead Alluvium. *Geosphere, 11*(1), 1–30.

Kasper Zubillaga, J. J., & Carranza Edwards, A. (2005). Grain size discrimination between sands of desert and coastal dunes from northwestern Mexico. *Revista Mexicana de Ciencias Geológicas, 22*, 383.

Kinsland, LG., Lock, EB. (2001). Proposed lower Colorado River courses prior to 4.3 Ma, Sonora, Mexico. In: Young, RA, Spamer, E (eds) Colorado River; Origin and Evolution, vol 12. Grand Canyon Association Monograph p 107–108.

Lonsdale, P. (1989) Geology and tectonic history of the Gulf of California. In: Winterer, E. L., Hussong, D. M., Decker, R. W. (eds) The Eastern Pacific Ocean and Hawaii, Geology of North America, Vol. N, p. 499–521. Geological Society of America.

Martín-Barajas, A., (2000), Volcanismo y extensión en la Provincia Extensional del Golfo de California. *Boletín de la Sociedad Geológica Mexicana* 53:72–83.

McDougall, K., & Miranda Martinez, A. Y. (2014). Evidence for a Marine Incursión along the Lower Colorado River Corridor. *Geosphere, 10*, 1–28. https://doi.org/10.1130/GES00975.1

McDowell, F. W., Roldán-Quintana, J., & Amaya-Martínez, R. (1997). Interrelationship of sedimentary and volcanic deposits associated with Tertiary extension in Sonora Mexico. *Geological Society of America Bulletin, 109*(10), 1249–1360.

Metzger, D. G. (1968). The Bouse Formation (Pliocene) of the Parker-Blythe-Cibola area Arizona and California. *US Geological Survey Professional Paper, 600*, D126–D136.

Miranda-Martínez, A. Y., Carreño, A. L., & McDougall, K. (2017). The Neogene genus Streptochilus (Brönnimann and Resig, 1971) from the Gulf of California. *Marine Micropaleontology, 132*, 35–52. https://doi.org/10.1016/j.marmicro.2017.2017.05.001

Nourse, J. A. (1989). Geological evolution of two crustal scale shear zones. Part I. The Rand thrust complex, northwestern Mojave Desert, California. Part II. The Magdalena metamorphic core complex, north central Sonora, Mexico. [Ph.D. thesis]: California Institute of Technology.

O'Connell, B., Dorsey, R. J., & Humphreys, E. D. (2017). Tidal rhythmites in the southern Bouse Formation as evidence for post-Miocene uplift of the lower Colorado River corridor. *Geology, 45*, 99–102.

Olmsted, F. H., Loeltz, O. J., & Irelan, B. (1973). Geohydrology of the Yuma area, Arizona and California. United States Geological Survey Professional Paper, v. 486.

Olmsted, F. H., & McDonald, C. C. (1967). Hydrologic studies of the lower Colorado River region. *JAWRA Journal of the American Water Resources Association, 3*, 45–58.

Oskin, M., & Stock, J. (2003). Pacific-North America plate motion and opening of the Upper Delfín basin, northern Gulf of California, Mexico. *Geological Society of America Bulletin, 115*, 1173–1190. https://doi.org/10.1130/B25154.1

Oskin, M., Stock, J. M., & Martín-Barajas, A. (2001). Rapid localization of Pacific-North America plate motion in the Gulf of California. *Geology, 29*, 459–462.

Pacheco, M., Martín-Barajas, A., Elders, W., Espinosa-Cardeña, J. M., Helenes, J., & Segura, A. (2006) Estratigrafía y estructura de la cuenca de Altar del NW de Sonora: implicaciones para la historia del delta del Río Colorado y de la cuenca Salton. Revista mexicana de ciencias geológicas 23:1-22.

Pérez-Tinajero, C. (2007). Sísmica de Reflexión en el Desierto de Altar, Sonora, México. [M.S. thesis]: Centro de Investigación Científica y de Educación Superior de Ensenada, Baja California (CICESE), México, 101 p.

Puente-Huerta, J. (2019). Estructura de un sector del norte de la Cuenca de Altar, Sonora, a partir de sísmica de reflexión 2D. [M.S. thesis]: Centro de Investigación Científica y de Educación Superior de Ensenada, Baja California (CICESE), México. 96 p.

Reyes-Martinez, C. S., González-Escobar, M., Montalvo-Arrieta, J. C., Tapia, F. V., & Jenchen, U. (2021). Extension in geothermal fields between the Imperial and Mexicali Valleys revealed by 2D seismic imaging and joint gravity-aeromagnetic modeling. *Geothermics, 89*, 101984.

Spencer, J. E., Constenius, K. N., Dettman, D. L., & Domanik, K. J. (2021). Identification of seasonal varves in the lower Pliocene Bouse Formation, lower Colorado River Valley, and implications for Colorado Plateau uplift. *Geosphere, 17*(6), 1745–1761. https://doi.org/10.1130/GES02419.1

Spencer, J. E., & Patchett, P. J. (1997). Sr isotope evidence for a lacustrine origin for the upper Miocene to Pliocene Bouse Formation, lower Colorado River trough, and implications for timing of Colorado Plateau uplift. *GSA Bulletin, 109*(6), 767–768.

Stewart, J. H., & Roldán-Quintana. (1994). Map showing late Cenozoic extensional tilt patterns and associated structures in Sonora and adjacent areas. US Geol. Surv. Misc. Field Studies Map MF-2238.

Stock, J. M., & Hodges, K. V. (1989). Pre-Pliocene extension around the Gulf of California and the transfer of Baja California to the Pacific Plate. *Tectonics, 8*, 99–115. https://doi.org/10.1029/tc008i001p00099

Sumner, J. R. (1972). Tectonic significance of gravity and aeromagnetic investigations at the head of the Gulf of California. *Geological Society of America Bulletin, 83*, 3103–3120.

Vega Granillo, R., & Calmus, T. (2003). Mazatan metamorphic core complex (Sonora, México): Structures along the detachment fault and its exhumation evolution. *Journal of South American Earth Sciences, 16*(4), 193–204.

Winker, C.D., Kidwell, S.M., (1996). Stratigraphy of a marine rift basin; Neogene of the western Salton Trough, California. In: Abbott, P., Cooper, J.D. (eds.) Field conference guidebook and volume, american association of petroleum geologists, Annual Convention, San Diego, CA: Bakersfield, CA, American Association of Petroleum Geologists, Pacific Section, and Society for Sedimentary Geology (SEPM), 80, 236–295.

Wong, M. S., & Gans, P. B. (2003). Tectonic implications of early Miocene extensional un-roofing of the Sierra Mazatán metamorphic core complex, Sonora, México. *Geology, 31*(11), 953–956.

Yilmaz, Ö. (2001). *Seismic data analysis: Processing, inversion, and interpretation of seismic data*. Society of Exploration Geophysicists.

(Received November 24, 2021, revised August 4, 2022, accepted August 19, 2022, Published online September 1, 2022)